NGT-21-002-080
NGT-80001

HQ GRANT
IN-01-CR
117P

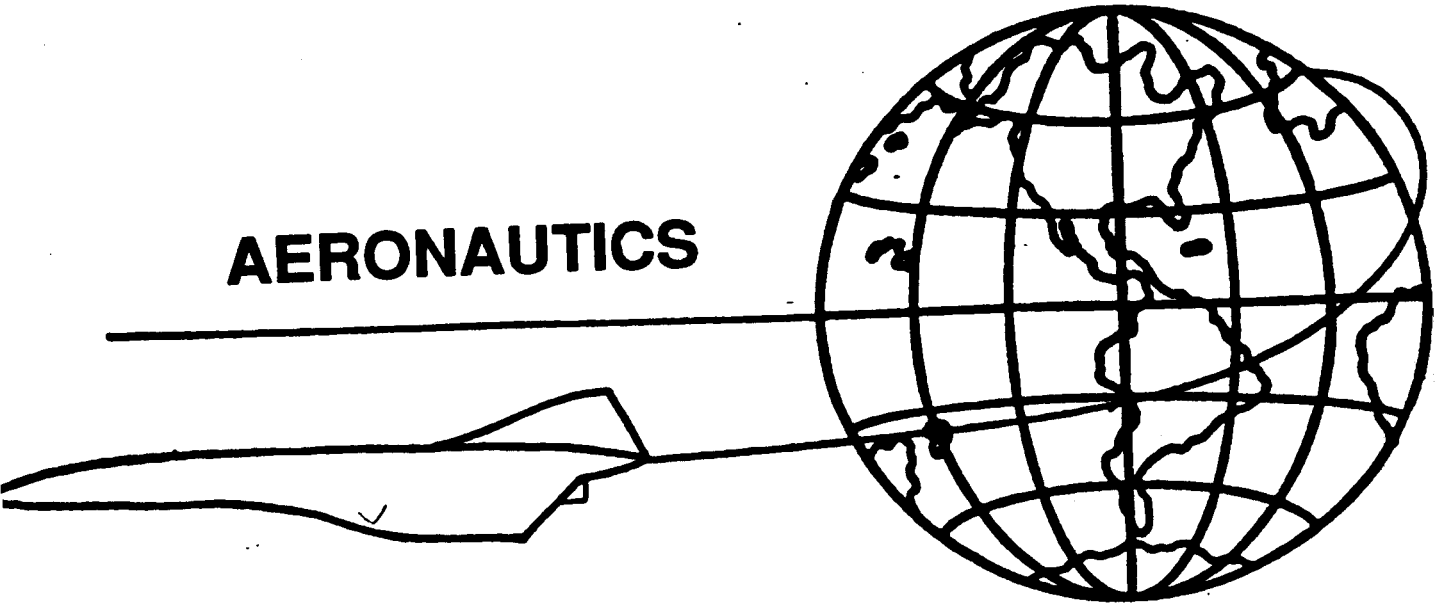

CALIFORNIA STATE POLYTECHNIC UNIVERSITY, POMONA

NASA / USRA ADVANCED DESIGN PROGRAM

JUNE 11, 1988

VOLUME 6

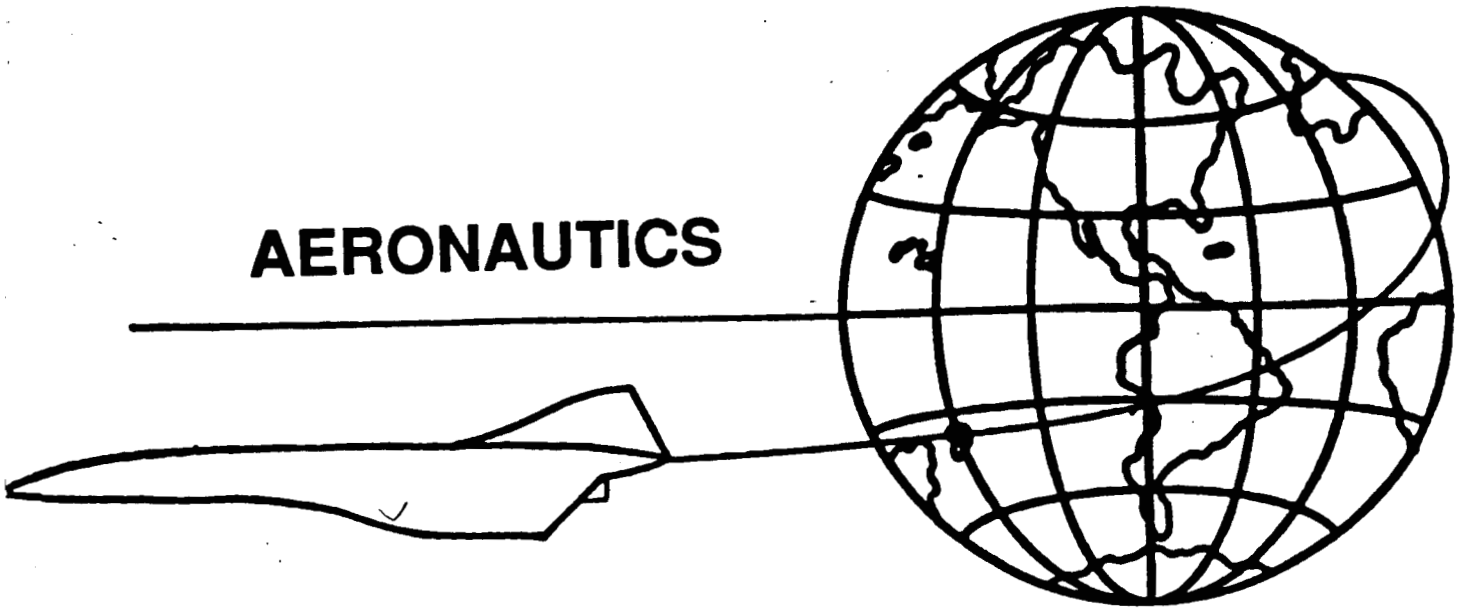

CALIFORNIA STATE POLYTECHNIC UNIVERSITY, POMONA

NASA / USRA ADVANCED DESIGN PROGRAM

JUNE 11, 1988

VOLUME 6

NASA/USRA Advanced Design Program

California State Polytechnic University, Pomona

Aerospace Engineering Department

Final Report 1987-88

ISAAC

Inflatable Satellite of an Antenna Array for Communications

Design Team Members:

Deborah Lodgard, Project Leader
Patrick Ashton
Margaret Cho
Tom Codiana
Richard Geith
Sharon Mayeda
Kirsten Nagel
Steven Sze

11 June 88

ABSTRACT

ISAAC is the result of the space team design as part of the 1988 AIAA/Allied Corporation Team Design Competition. The request for proposal for this design was for an antenna array satellite using rigid inflatable structure (RIS) technology. ISAAC, an Inflatable Satellite of an Antenna Array for Communications, meets the design criteria as specified in the request for proposal.

An inflatable satellite allows for a very large structure to be extremely compacted for transportation in the Space Shuttle to the Space Station, where it is then assembled. An antenna array allows for the construction of many small antennas, which can then have an equivalent aperture of a single antenna of any size, which can also be pointed electronically at different targets.

The initial design, ISAAC, is a communications satellite for two-way communications with many low-power stations on the ground. The total weight was determined to be 15,438 kg, which is under the allowable limit of the Space Shuttle. It will have an equivalent aperture greater than 100m in diameter and will be operable in K and C band frequencies, with a total power requirement of 10,720 watts.

The cost of the structure was determined to be approximately 350 million dollars, but the cost performance is as low as 93,000 dollars per transponder year. Furthermore, the techniques of this design can be easily extended so that ISAAC could be used for many other missions.

TABLE OF CONTENTS

FIGURES

TABLES

1.0 INTRODUCTION

One of the primary functions of the Space Station is to be an orbiting base from which large space structures can be built and then deployed to other locations in space. This is very helpful for very large satellites, for the primary components can be cleverly packaged into the Space Shuttle cargo bey, and it can then be assembled at the Space Station.

This particular Request for Proposal (RFP), as part of the 1988 AIAA/Allied Corporation Team Design Competition, is for an antenna array satellite using rigid inflatable structure (RIS) technology. Using RIS technology combines the extreme compactness of an inflatable structure with the rigidness of a structure that is assembled in orbit from rigid components. The initial structure can be packaged into the Space Shuttle cargo bay, and then it is brought up to the Space Station. Once there, the structure is inflated, and then it undergoes a curing process to rigidize it. The gas is leaked out, and the result is a non-pressurized, very large structure that can sustain impact from micrometeorites with no major structural damage. It can then be deployed into geosynchronous orbit, where the satellite is fully operation.

Using an antenna array allows for the construction of an antenna with any desired size. Furthermore, the array will have not only the equivalent aperture of a single

antenna, but it will also have the capability to be pointed electronically at different targets without repositioning the whole satellite. Thus, having a phased array of many smaller antennas can be very advantageous.

The design requirements and constraints put forth as part of the competition are as follows:

1) Complex, precision structures should be easy to package into minimum volumes while in the flexible state.

2) They must be easily inflatable in a zero- or micro-g environment using an environmentally safe, nontoxic gas.

3) "Curing time" must be comfortably less than the time for the inflation gas to leak from the structure. Once cured, the RIS structural properties should not change significantly with time (especially changes in size, shape, strength, and modulus of elasticity).

4) Finished structures must be able to withstand typical propulsion stresses during orbit change from the Space Station orbit to the operational geostationary orbit.

5) In operation, the RIS must retain a sufficiently precise shape to do the mission properly despite uneven thermal heating and mechanical loading.

6) A RIS structure should be able to tolerate micrometeorite impact without failing or causing significant structural deformation.

7) If surface coatings or coverings are required by a RIS application, they should be incorporated into the original nonrigid flattened-out package so that they will not require application or installation subsequent to the structure's inflation.

The result of these requirements and constraints is ISAAC: an inflatable satellite of an antenna array for communications. ISAAC will be constructed using RIS technology for both the antenna array and the satellite that is to carry the array, and it meets all the requirements put

forth. It will have an equivalent aperture greater than 100 m in diameter, and its initial design is as a satellite for two-way communications with many low-power stations on the ground. However, the techniques can be extended so that it can be used for other missions, such as for television use, radio interferometry, weather studies, or even as a power satellite.

2.0 CONFIGURATION

To meet the requirements and constraints put forth in the RFP, the configuration was designed so that the satellite structure would be fully inflatable. Furthermore, although the RFP allowed for the antenna surfaces to be pre-finished, it was decided to use RIS technology for them, also.

2.1 Overall Configuration

For the initial design, two different configurations for the communications structure were considered. In the first, the many small reflectors would be connected together to form one large parabolic reflector with a 100 m diameter. Each piece would have its own integral support structure so that when all the parts are connected, one large structure is formed. Extended from the edge would be a boom with all the antenna feeds positioned at the focal point. By moving the feeds on the boom, the beamwidth of signals could be changed to give either global coverage or spot coverage of a selected area. The second configuration consisted of many small reflectors with individual feeds mounted directly to them. These reflectors would then be mounted on a separate support structure that would include the necessary interconnection equipment. This way, each reflector could be individually configured for transmission or reception of a specific beamwidth and frequency. This latter configuration was the

one we chose because it more adaptable to the different mission profiles called out in the Request for Proposal.

After deciding upon this configuration, it was necessary to know how many reflectors would be needed to meet the 100 m effective diameter requirement. Since the reflector concentrates a dispersed signal to a receiver, the effective diameter of many small reflectors would be the diameter of a reflector with the same area as all the small reflectors combined. Therefore, for an average 10 m diameter reflector, 100 reflectors would be needed to have an effective diameter of 100 m. From the plot in Figure 2.1, it can be seen that for the 12 m reflector used in our design, a minimum of 70 reflectors are needed for a 100 m effective diameter.

For the reflector, it was decided to use offset fed parabolic reflectors instead of the common center fed reflector because it would eliminate interference from the feed support and increase the signal to noise ratio of the receiver. To mount the reflectors, the design shown in Figure 2.2 was developed. In this configuration four inflatable, offset fed reflectors would be connected to a common base like a four leaf clover, thus reducing the number of mounting points needed on the support structure. Feeds for the reflectors would be located on a common support boom extended from the central control module allowing the four to operate either as one or separately. Although this configuration requires more room than an equivalent size center feed reflector, it could be packaged in the same space

and would be easier to deploy during assembly in orbit.

For the support structure on which the reflectors would be mounted, a configuration was initially selected which had thirty-seven subassemblies placed in a hexagonal pattern as shown in Figure 2.3. Each subassembly would be connected to the subassemblies adjacent to it by an inflatable truss structure 25 m long for an overall length of 150 m. This configuration was later abandoned when initial mass calculations showed the structure to be too heavy.

The design was replaced with a toroidal structure shown in Figure 2.4. The idea for a torus shaped configuration came about mainly from a desire for simplicity. This is a fundamental driving force when reliability is a high priority. Though the initial configuration was very ingenious and could be tightly packaged, it was too complex and massive. Failure of a single component to unfold and deploy correctly could have jeopardized the entire mission.

Another key factor which contributed to the decision to go with the torus structure was the desire to have a symmetrical object. This would make the load on the structures group much easier to handle in the time frame available as only one section would need to be analyzed. Additionally, a symmetrical structure would be much easier to stabilize.

Initially, the design consisted of one circular ring with all the antenna groups placed on the circumference. This design was rejected by the structures group as being

unstable because of the large diameter of the torus required to place all of the groups on the circumference. The logical answer to this problem seemed to be to add cross members to support the structure. Therefore, one horizontal and one vertical cross member were added which met in the center on a hub where the control center would be located. The diameter was unchanged and as all the antenna groups remained on the circumference. The structures group agreed that the design was feasible and worth analyzing, but the weights person said that the design was too massive. The density of the RIS material was given as a mass per unit area and a great deal of surface area was being used for the cross members, as is shown in Figure 2.5. As can be seen, it is not practical for the circumference to be required to support 100 percent of the antenna groups when it is composed of only 61.1 percent of the surface area.

The answer to the problem appeared to be obvious: place some of the antenna groups on the cross members. This would allow the radius of the circumference to be reduced, thus reducing the structural mass. The groups would have to be moved in groups of four to preserve symmetry. The plot shown in Figure 2.6 shows that the best choice was to move a total of eight groups of antennas onto the cross members. As can be seen, the critical radius is that of the cross members as it is greater than the radius required by the circumference to support the remaining sixteen antenna groups. Figure 2.7 shows that the percentage of antenna groups located on the

cross members (33 percent) now compares quite well with the surface area being used by the cross members. For these reasons the design was set to this configuration.

Thus, the configuration consists of an outer ring 150 m in diameter, with four arms extending from the center to the ring. To this structure, twenty-four reflector subassemblies would be mounted, two on each of the four arms and the remaining sixteen equally spaced on the outer torus. All attitude and command control for the satellite would be located at the center module with altitude control thrusters located at the intersection of the four arms and the outer ring. Two solar array panels will be attached to the outer ring at opposite sides where they can be rotated to point at the sun. Instead of the truss structure used in the first configuration, the outer ring and central arms would be a single inflatable tube. This simplifies the design and will reduce fabrication costs tremendously. Substantial space is also saved in the stowed configuration by having the reflector subassemblies attached to the structure after it has been inflated and cured.

2.2 Main Structure

At the center of the main structure will be the command module. Made primarily out of aluminum, this 3 m cube will house all the command and control electronics for the whole satellite as well as the power storage batteries. It will

also have an interface connecting the pressurization hose receptacle to the four radial arms. Where the radial arms intersect the main toroid will be four thruster modules. These 2 m cubes will house the propellant tanks and nozzles for the attitude and control thrusters. They will also have electrical and pressure connections linking the radial arm to the toroid. Two of these will also have attachment points for the two solar panels. The main toroid and four radial arms will be connected to the command and thruster modules by attachment rings bonded to the ends of the material. Electrical connections from the command module to the thruster modules and the reflector subassemblies will be through cables lining the arms and toroid. The total mass for the whole assembly is estimated at approximately 1000 kg.

2.3 Reflector Subassembly

As stated previously, there will be twenty-four reflector subassemblies, each with four 12 m diameter reflectors. Thus, the equivalent aperture is greater than 100 m in diameter, which exceeds the RFP requirement. Again, all the reflectors will be constructed using RIS technology.

2.3.1 Configuration

At the center of the reflector subassembly is the control module shown in Figure 2.8. This is a 0.8 by 0.8 by 1 meter tall container in which all the communications and control equipment will be located. This module will be constructed from aluminum for maximum weight savings with an

external coating to protect the electronics from radiation. Initial estimates place the mass of the control module at 50 kg with another 50 kg allotted for communications equipment. Adding to this the 63 kg mass of each reflector gives a total mass of 352 kg for the subassembly.

The reflector used in the configuration is a 12 meter, offset antenna reflector using inflatable space rigidized structure, under development by Contraves Corp., Zurich, Switzerland [Reference 4]. The design (see Figure 2.9) consists of a 12 m diameter stabilization torus bonded to an RF-reflective, quasi-elliptical lens on the bottom and an RF-transparent lens on the top. The reflector is connected to the support structure by a solid torus segment in the plane of symmetry. This aluminum interface also contains the connections between the inflatable chamber and the pressure control unit. Before deployment, the reflector will be stowed in a protective container consisting of an aluminum back plate with a hinged cover. This container will restrain the flexible structure during transport as well as protect the prepreg ISRS from excessive mechanical and thermal loads up to the deployment time.

From an analysis by Contraves Corp. [Reference 5], the mass breakdown for the 12 m offset-fed reflector is as depicted in Table 2.1.

Table 2.1 Reflector Mass Breakdown

Main Chamber	42.25 kg
Torus	7.26 kg
Pressurization Subsystem	4.29 kg
Stowage Elements	10.34 kg
Total Mass	63.14 kg

From an analysis of the membrane force, a minimum ratio of torus pressure to main chamber pressure of 1072 was calculated. Pressure tests on the scale mockup show that the nominal pressure for the main chamber was 20 Pa, with a corresponding torus pressure of 60 kPa. Since it was decided to use boron trifluoride gas, the requirement is 0.6 g to inflate the main chamber and 78.6 g for the torus. Thus the total mass needed to inflate the 96 reflectors is 7.6 kg.

Manufacturing errors for the full size reflector, shown in Table 2.2, were predicted with a model developed from data measured from a 23% scale mockup [Reference 5].

Table 2.2 Reflector Manufacturing Errors

Aperture	10 m	10 m	20 m	
F/D	0.65	0.32	0.65	
W_{RMS}	0.3	0.9	0.5	mm
Defocus	1.1	0.6	2.2	mm
D/W_{RMS}	35000	22000	39000	
Frequency (-0.6 dB)	20 GHz	6.7 GHz	12 GHz	

From this, it can be seen that the RMS error is more

dependent on the F/D ratio than on aperture size.

This reflector was chosen because, compared to other deployable antenna currently being used, the ISRS reflector displayed characteristics comparable to most of them, and even better performance in some areas. The ISRS antenna would be as light as a mesh antenna, as rigid as a light-rib antenna, as resistant to thermal distortion as panel element structures, while at the same time, having a packaged volume less than any other antenna. With material technology evolving and improvements in design optimizations, the ISRS antenna will have a place in space structures far into the future.

2.3.2 Manufacture

In their analysis of the inflatable, offset fed reflector, Contraves divided the manufacturing process into three parts. The first is the fabrication of the prepreg and laminate foils to be used in the finished reflector. Next is the manufacture of the toroidal ring and curved radome and reflector surfaces. Last is the bonding together of the components into the final reflector assembly. Fabrication of the stock materials would be done by the suppliers according to the specifications supplied. For the manufacture of the reflector and radome membranes, a manufacture and integration jig (MIJ) was developed for improved accuracy. The MIJ uses a parabolic shaped swiveling trolley to support the membrane gores while they are bonded to each other and to the toroidal

rim. The torus, manufactured separately, is held in place by the toroidal holding tool. The membrane gores are initially cut from a flat laminate to reduce complexity while toroidal gores are preshaped. The toroidal gores are first laid up in the toroidal holding tool and bonded using prepreg strips as doublers. Then, a torus is positioned in the tool and inflated, pressing the prepreg segment into shape. The membrane gores are supported in the trolley and bonded to the toroidal segments one at a time until the surface is complete. After both membranes have been assembled, the torus is deflated and removed from the holding tool. A preshaped toroidal sealing foil is then fitted around the outer segment and the gore junctions are taped to complete the sealing layer.

2.4 Packaging

As stated in the RFP, a primary advantage to using rigid inflatable structures is that they can be stored in less space when deflated than an equivalent solid structure. Since the structure retains the flexibility of the fabric its made of until it's cured, it needs some sort of protective cover to secure it in place. In order to make the most use of its space saving advantage, the reflectors and main structure should be folded in such a way as to reduce the size of their protective containers.

2.4.1 Folding Patterns

The bulk of the main structure is the central control module, which is 3 meters to a side, and the four thruster modules which are 2 meters to a side. Since the shuttle bay is only 4.5 meters in diameter, it is not enough just to push the thruster modules up against the control module. Instead, the folding pattern shown in Figure 2.10 is used, where two of the thruster modules are placed on top of the control module and the other two are placed on the bottom of the module. The inflatable torus is folded flat in an s shape so that it is only two meters wide. It can then be folded accordion style, allowing it to lie flat against the side of the control module. The whole assembly is then placed in a cylindrical cover, four meters in diameter, which holds the fabric up against the control modules. This cover is also used to secure the assembly to the holding rack in the shuttle bay.

To store the reflector in the container previously described, two series of folds shown in Figure 2.11 will be used. First, a series of lateral folds are made about the interface segment, so that each side overlaps the other. This reduces the number of sharp folds each side is subjected to, thus minimizing any creases in the fabric. Then the end is rolled towards the interface segment so that the overall length is just under the length of the container. This folding pattern also provides for easy unfolding in the micro-g environment of space. Once the reflector is folded, the protective cover is closed and the subassembly is ready

for launch.

2.4.2 Transport Configuration

Once all the components are assembled on Earth, they must be transported to the space station where they will be assembled into the final configuration. Since the components cannot be placed in the shuttle cargo bay loose, a rack will be used to hold all the components in place. This rack is shown in Figure 2.12. Another advantage with using the rack is that it can be removed and attached to the space station, freeing the shuttle to return to Earth for another mission. Constructed out of tubular aluminum, the rack will extend the full length of the shuttle bay. The forward seven meters will hold the main structure. The structure will be stowed as previously described and placed inside a protective shroud which will be secured to the side of the rack. The next five meters will hold the 24 reflector subassemblies and the two solar panels. The subassemblies will be stacked three wide and three high in two rows with a third row only two high. The solar panels will sit on top of the third row. The last eight meters will contain the barium trifluoride tank, pumps, hoses, and other equipment for inflating the satellite. The rack will be secured to the shuttle bay by mechanical catches which will be released at the space station, allowing the remote manipulator arm to lift the rack from the bay and transfer it to the space station. There, it will be secured to the space station structure by the same mechanical catches.

2.5 Deployment

Once the structure is secured at the Space Station, it is ready to be inflated and assembled. The inflation process will basically consist of two phases. The first involves the main structure, and the second involves the reflector subassemblies.

2.5.1 Main Structure

The first part to be removed from the transportation rack will be the main structure. Once it is removed from its protective shroud, it will be moved to a position approximately 300 m from the space station. Here, it will be spread out by four astronauts to closely resemble its final shape.

Once the torus structure is spread out of the shuttle bay into its approximate shape, the inflation process can begin. The inflation gas, boron trifluoride, will be stored in a tank attached to the space station. There will be four three hundred meter, 2.54 centimeter diameter hoses attached to the tank. The hoses will be taken by the astronauts to the center of the torus structure and attached to the bases of the cross members by using the inflation valves shown in Figure 2.13. The valve openings used will be 1.91 cm in diameter. Once the hoses are connected, the astronauts will have to retreat to the safety of the space station while inflation occurs. When the sun just begins to appear over

the horizon, the inflation of the main structure to a pressure of 60 kPa will occur.

Once fully inflated, the astronauts will emerge and retrieve the hoses. The structure will then be allowed to cure while exposed to the sun for a minimum of six hours. After the structure becomes rigid, the attitude control system will be activated. The attitude control system can be used to stabilize the structure during the delicate process of attaching and inflating the antenna groups. Once the attitude control system is functioning, the antenna groups can be attached to the structure. This process should take approximately twenty four hours for crews of two astronauts working at one time. Once all the module are attached to the main structure, antenna inflation will begin. To preserve the symmetry of the structure, four antenna groups will be inflated at one time. For instance all four inner cross member group, then all four outer cross member groups, etc. Therefore, all four boron trifluoride hoses must be attached to the four antenna groups and then all four will be inflated simultaneously. The astronauts will have to take cover in the space station before inflation can occur just as in the case of the main structure. Once inflated, the hoses will be disconnected from the groups and then reconnected to the next set of four groups, however inflation of these groups will not occur until the previous groups have fully cured. Using this method, the total time to inflate all of the antenna

groups will be roughly five days.

2.5.2 Reflector Subassemblies

Each reflector subassembly will be attached to the main structure by two lock down mechanisms fabricated into the sides of the toroid, and two guides located on the top. After the subassembly is moved into position, two short legs extending from opposite corners of the control module are inserted into the guides on top of the torus. Then two longer legs on the other corners are inserted into holes in the top of the lock downs until small bearings drop in a grove in the end of the leg. Then a handle on the outside of the unit is turned one quarter turn driving a pin through the leg, locking it in place. At this point, a connector in the bottom of the control module is plugged into a receptacle in the main structure, connecting it to the main controls and power source. After a test of the electronic components, the antenna feed boom will extend from the top indicating that all systems check out okay. Once the subassembly is secure, small rings in the top of the control module are pulled, releasing the reflector storage containers. Small, hydraulically operated scissor arms extend the container to the deployed position where wires at each corner of the box hold it in place. The gas storage tank is connected to the pressurization subsystem by a quick connect hose assembly same as was used to inflate the main structure. The reflectors can then be released from their containers and inflated to the required pressures. Again, the reflectors

should be released from their protective containers only while the space station is in the Earth's shadow to prevent premature curing of the RIS material.

2.5.3 Inflation Gas Tank

The amount of boron trifluoride (BF_3) required to inflate the structure and antennas is 100 kg. The four, 300 meter hoses can hold 4.1 kg of gas. Ten percent extra gas will be brought along for excess, in case of leakage or other unforeseen problems, which will bring the total gas mass up to 114.5 kg. In order to push all of the BF_3 into the structure at 60 kPa, the initial pressure in the storage tank will need to be 1.1 MPa. Assuming the gas is to be stored at 293 Kelvin for preliminary design, this yields a tank volume of 3.43 cubic meters. A cylindrical pressure tank will be used with an inside diameter of 0.75 meters and an overall length of 2.44 meters. Using aluminum with a working stress of 36 MPa for preliminary design, the required tank thickness is 2.5 cm and the tank will have a mass of 801.31 kg. The total mass of the inflation system will be 920 kg at liftoff.

Figure 2.1
EFFECTIVE DIAMETER
OF MULTIPLE REFLECTORS

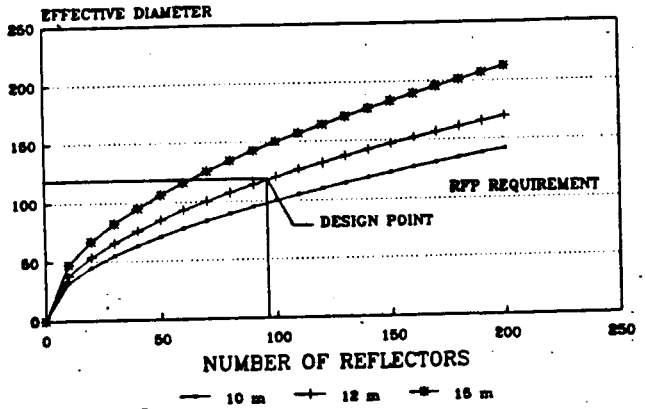

Figure 2.2
REFLECTOR SUBASSEMBLY - DEPLOYED

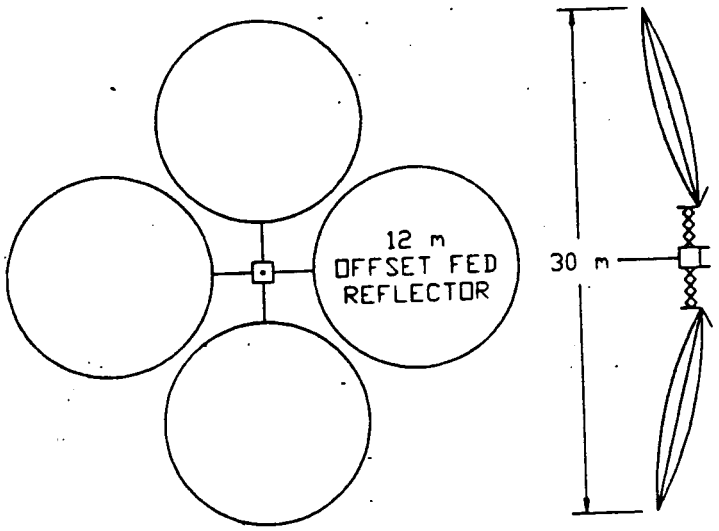

Figure 2.3
PRELIMINARY CONFIGURATION

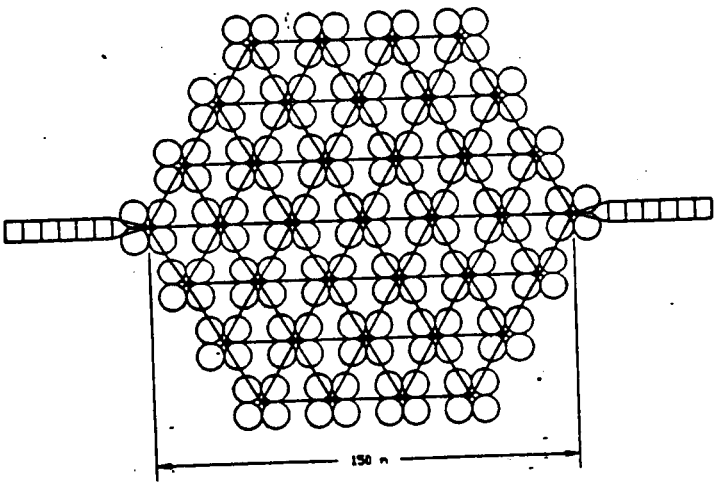

Figure 2.4
SATELLITE CONFIGURATION

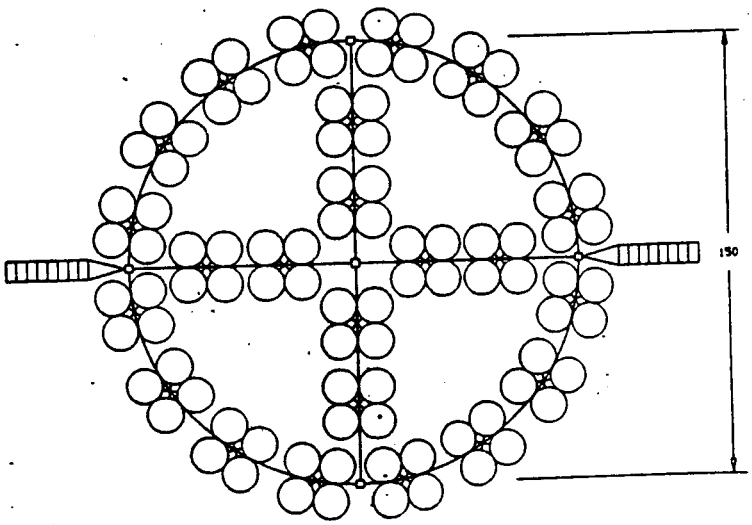

Figure 2.5

Relative Surface Area of Cross Members and Circumference of Torus

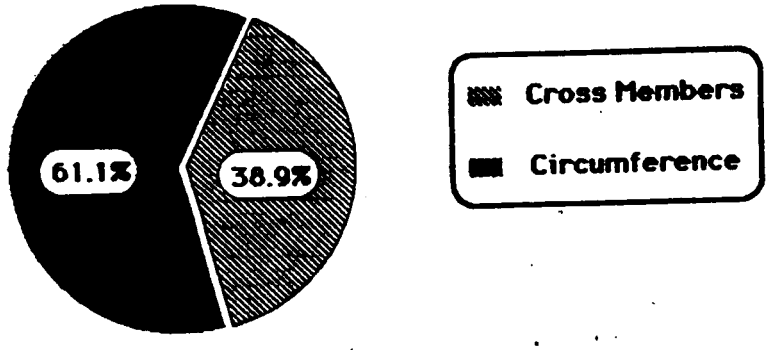

Figure 2.6

Required Radius for Cross Members and Circumference as a Function of the Number of Antenna Groups Located on the Cross Members

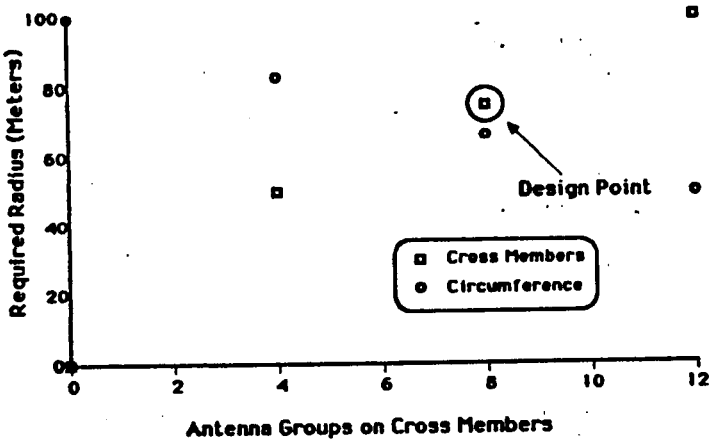

Figure 2.7

Percentage of Antenna Groups Located on Circumference and Cross Members

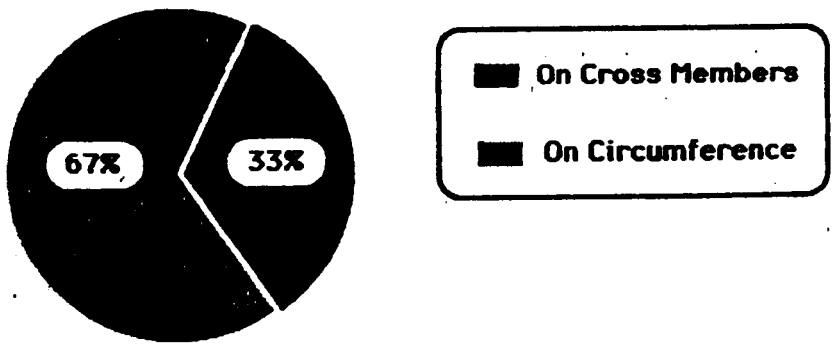

ORIGINAL PAGE IS
OF POOR QUALITY

Figure 2.8

REFLECTOR SUBASSEMBLY (STOWED)

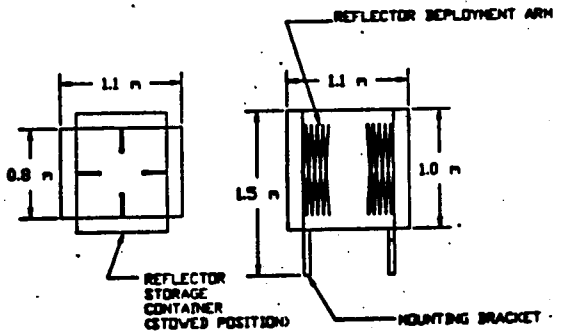

Figure 2.9

12 m OFFSET FEED REFLECTOR

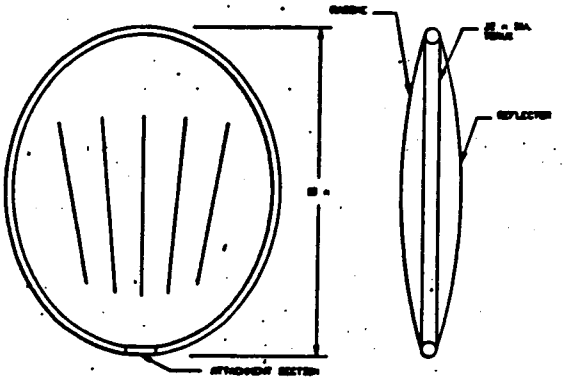

Figure 2.10

MAIN STRUCTURE - STOWED CONFIG.

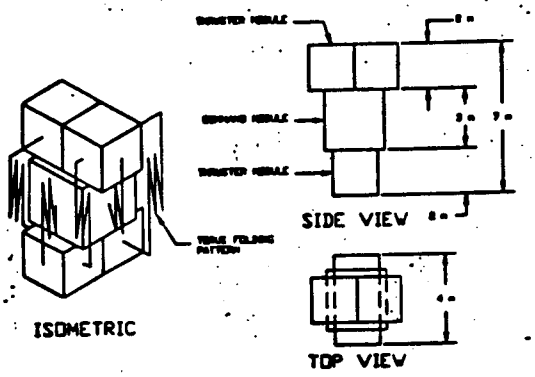

Figure 2.11

REFLECTOR FOLDING PATTERN

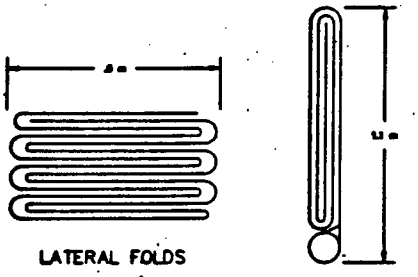

Figure 2.12

SHUTTLE STORAGE CONFIGURATION

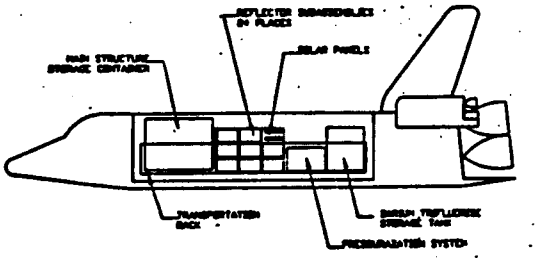

Figure 2.13

Inflation Valves

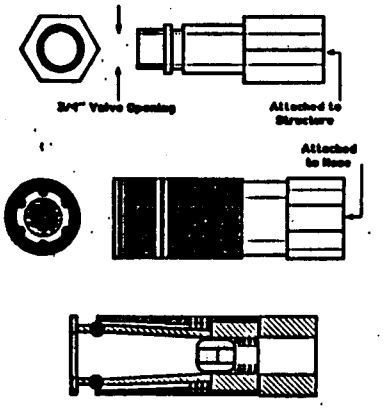

3.0 SPACE ENVIRONMENT

To place our designed spacecraft into the geostationary orbit (GEO), we first have to understand the environment in that region. For example, we have to familiarize ourselves with which things are hazardous and which things are advantageous to us. From recent studies, the GEO has already proven to be a popular place to place satellites, therefore, selection of where to park this large structure needs to be dealt with very carefully. Besides the problems which humans have caused, there are problems which nature has created also. They are, mainly, ultraviolet radiation, solar flares, micrometeorites, spacecraft charging and thermal effects in space.

3.1 Radiation

Sunlight in space is far more intense than at the surface of the earth. This is due to the lack of atmosphere absorption. The intensity is especially strong at shorter wavelengths, because the energy of a photon is inversely proportional to its wavelength. Therefore, ultraviolet photons are more energetic than those of visible light (Figure 3.1). Such a great intensity of solar ultraviolet in space can be very damaging to materials and living tissues [Reference 28]. Obviously, some kind of special coating is needed to protect the spacecraft. (This will be discussed in Section 4.4.5.)

3.2 Solar Flares

The sun is very active magnetically, and its magnetic phenomena include the sudden release of energy stored in the magnetic fields in such a way as to accelerate charged particles to very high energy. Flares are random events, and cannot be predicted in advance, but there is a long term correlation with sunspot cycle (Figure 3.2). The radiation from a flare event lasts only few days [References 10 and 16], but, needless to say, protective means is a must.

3.3 Micrometeorites/Manmade Debris

Micrometeorites are small, metallic particles. Fortunately they are small, about the size of a grain of sand, but they can weigh a lot. The punctural effect of the solid particles (micrometeorites or manmade debris) on the spacecraft is not only structural failure, but also the erosion of the exposed surface. Still, the danger from puncture has been found to be secondary to erosion hazards. Micrometeorites have a density around 0.5 g/cm^3 and are traveling at approximately 20 km/sec. Therefore, they are invisible and unavoidable. Also, manmade debris has density from around 2.7 to 8.0 g/cm^3. It has been estimated that there are approximately 600 trackable objects and about 2,000 smaller debris at GEO. Damage from impact due to large debris or large micrometeorites are unfortunate , but damage due to smaller debris can be protected by using a good set of coating materials on the outside surface of the spacecraft [Reference 10].

3.4 Spacecraft Charging

Spacecraft charging is a phenomenon related to trapped electron activity near geosynchronous orbit. At this altitude, magnetic turbulence frequently arises from the magnet fields of the Sun and Earth. During these periods, the electrons carried by the turbulence can interact with an orbiting structure. This interaction can cause differential charging between solar illuminated surfaces which can dissipate charge by emission of photoelectron, and unilluminated surfaces which cannot. If a voltage difference is large enough, arcing can be created, resulting in physical damage to the spacecraft. This problem can be reduced by using a proper set of surface coating [Reference 28].

3.5 Thermal Effects in Space

The temperature of a spacecraft in space is determined by the balance between the heat gained by direct radiation from the Sun, and the heat radiated away from the body surface. Also, the temperature reached by a spacecraft depends on its surface finish and weather it is in the sunny side or in the Earth's shadow. Still, no matter how hot or cold the outside of the spacecraft might be , the equilibrium temperature of the spacecraft must be kept within -150 ° C to 150 ° C [Reference 1]. A variation of surface properties ith the equilibrium temperature is depicted in Figure 3.3.

Figure 3.1

SOLAR RADIATION SPECTRUM

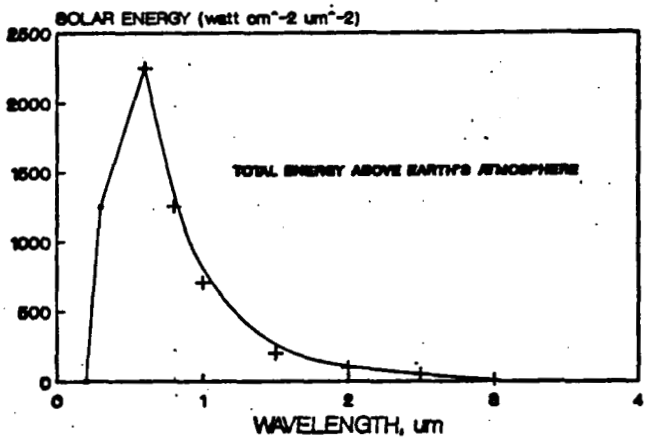

Figure 3.2

SOLAR ACTIVITY

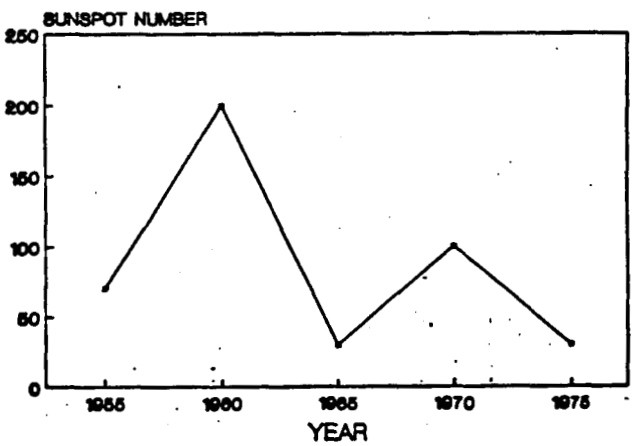

Figure 3.3

SURFACE PROPERTY vs. EQUILIBRIUM TEMP.

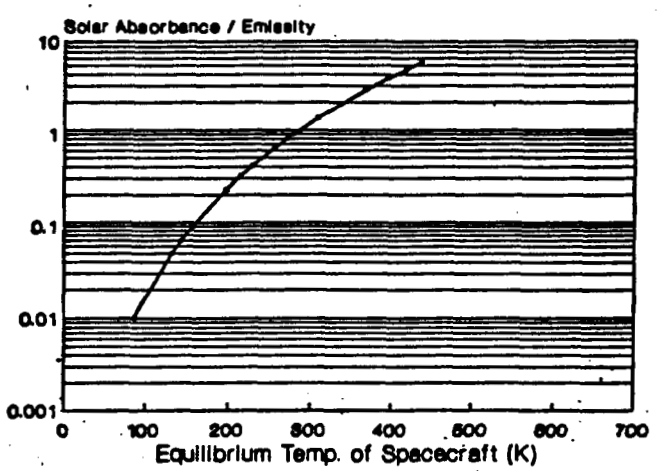

4.0 MATERIALS

The RFP defines the requirements which a RIS structure must meet, which seem to allow for the space environment. Using these requirements, the specifications for the materials can be defined, which then leads to the selection of which materials to use. An analysis is them performed to verify the validity of the selection and to show that the specifications set by the RFP and the space environment are met.

4.1 RIS Requirements

The requirements of a satellite using rigid inflatable structures are:

1. Designed for a space environment.
2. Offer a good package ratio.
3. Simple to deploy
4. Dynamic characteristics are excellent.
5. Have relatively low thermal distortions.
6. Antennas are geometrically accurate.
7. Low cost.

Inflatables are designed for the space environment. They are manufactured on the ground, packaged into the space shuttle, and deployed into space. The package ratio of the inflatable satellite is very good. Deployed, the structure is very

large, but when packaged the structure is very small in comparison. Deployment is very easy, since there are not a lot of mechanics necessary to power or control deployment. The dynamic characteristics of the inflatable satellite are also very good. The structure is a closed membrane, and therefore the ratio of area mass to membrane stiffness is small. Furthermore, inflatables have relatively low thermal distortions.

Since the structure is a closed cavity, the heat transfer substantially decreases the temperature gradients in comparison with open surfaces. Also, the inflatable antennas are geometrically accurate, in which a double curvature surface is created by shaping pressures. Almost most importantly, though, is that inflatables are low in cost. The inflatable satellite is of lower cost than other satellites because of its small package ratio, ability to be constructed on the ground, and the overall structure is lighter and therefore easier to deploy.

4.2 Material Requirements

From the satellite requirements the materials' requirements can be determined. The material properties for the reinforcement are:

1. Elasticity Modulus 9 - 40 GPa
2. Ultimate Strength 200 - 600 MPa

The material properties of the resin are:

1. Tensile Stiffness 0.63 - 2.80 MN/m

2. Ultimate Strength 14 - 42 KN/m

The material properties for the composite are:

1. Coefficient of Thermal Expansion 5 $\frac{\text{microstrains}}{\text{Kelvin}}$

2. Wall Area mass 0.1 Kg/sq. m

3. Storable for a reasonably long period.

4. High flexibility.

5. Not tacky or sticky.

6. Cures easily.

7. Cured product should not degrade under space conditions.

The composite needs to be able to be stored for a reasonably long period. This is because the structure will be folded up in the Space Shuttle for transportation. Therefore the folded structure must be able to withstand the duration it takes to orbit the shuttle without destroying the product. The composite must also have high flexibility so that it can be folded, and it must not be tacky so that once it is folded it can be unfolded without sticking to itself. Furthermore, the composite must cure easily, and the curing process must be quick and easy to perform. The reason for this is that there are limited resources in space for any kind of elaborate curing process. Furthermore, the cured composite

should not degrade under space conditions, which means it should stand up to temperature gradients and space particles [Reference 9].

4.3 Analyses of Materials

There were three fiber reinforcements that could have been chosen to be used for the structures, each with its own benefits. Furthermore, there were also many resins to choose from. Thus, each of the materials were analyzed so that a decision could be made on which materials to select.

4.3.1 Reinforcement

Three fiber reinforcements were analyzed: 1. Synthetics, 2. Glassfiber, and 3. Kevlar. Synthetics possess low tensile modulus, moderate strength, and large coefficients of thermal expansion. Glassfiber has a substantial tensile modulus, is strong, and has a reasonable coefficient of thermal expansion values. Kevlar has a high tensile modulus, high strength, and low coefficient of thermal expansion values.

4.3.2 Resin

Four resins were analyzed: 1. resin D (Araldite LZ 580-A-80/HT 973), 2. resin E (LMB 2436), 3. resin G (LMB 2802/2803), 4. resin H (LMB 2804/2805). Resin D is a cycloaliphatic, laminating resin. It is catalytically cured. Once cured it has good UV stability, good resistance to thermal degradation, and allows a change in reactivity

without changing the properties of the cured composite. It also has low a volatile content. Resin E is an acrylic resin. This material has good flexibility and is transparent. Resin E can be thermally or UV cured. Resin G is a combination of resins B and F. This resin is an amide-cured, epoxy, thermoplastic polyimide, laminating resin. Resin G has low volatility in vacuum and rigidizes in space by physically drying. Resin H is a combination of Resins D and F. This resin is a catalytically cured, cycloaliphatic, thermoplastic polyimide, laminating resin. It also has a low volatile content, improved UV stability, and good resistance to thermal degradation. It allows for a change of reactivity without changing the properties of the composite and rigidizing in space by physically drying.

4.4 Selection of Materials

Several materials were chosen to be used on the satellite. The materials chosen for the reflector and radome are depicted in Table 4.1, while the materials chosen for the antenna torus and the main structure toroid are depicted in Table 4.2 and Table 4.3, respectively.

Table 4.1. Materials Chosen for Reflector and Radome

KEVLAR 49	- FIBER REINFORCEMENT
LMB 2804	- RESIN MATRIX
KAPTON	- PLASTIC FILM SERVES AS A GAS BARRIER

METTALLIC ALLUMINUM	- LAYER APPLIED TO REFLECTOR SHELL
INDIUM TIN OXIDE	- LAYER APPLIED TO RADOME SHELL
LMB 2805	- GASEOUS CATALYST FOR CURING
BF_3	- GAS USED FOR CURING

Table 4.2. Materials Chosen for Torus

POLYESTER CLOTH	- REINFORCED BY KEVLAR RADIALLY APPLIED POLYURETHAN BLADDER

Table 4.3. Materials Chosen for Toroid

KEVLAR 49	- FIBER REINFORCEMENT
LMB 2804	- RESIN MATRIX
KAPTON	- PLASTIC FILM SERVES AS A GAS BARRIER
INDIUM TIN OXIDE	- PROTECTIVE COATING
LMB 2805	- GASEOUS CATALYST FOR CURING
BF_3	- GAS USED FOR CURING

4.4.1 Reinforcement

Selection of the reinforcement was determined by which material had the highest tensile modulus, highest strength, and lowest coefficient of thermal expansion value. Kevlar is the material that has these attributes. Still, there were two Kevlars to choose between, Kevlar 29 and Kevlar 49. However, Kevlar 49 was chosen to be the reinforcement for the

composite, based on the following attributes:

1. High Tensile Strength.
2. High Tensile Modulus.
3. Elongation to break is low.
4. Low weight.

Figure 4.1 shows a stress versus strain curve for the Kevlar fiber, which reflects its high tensile strength, and Table 4.4 lists its actual material properties [Reference 11].

Table 4.4 Kevlar Properties

DENSITY	1.44 g/cm3
TENSILE STRENGTH	3620 MPa
TENSILE MODULUS	124 GPa
ULTIMATE ELONGATION	2.5 %
SPECIFIC HEAT	1380 J/kg C
LONGITUDINAL COEF OF THERMAL EXP	-6.3 E-6 m/mK
YIELD STRENGTH--compression	221 MPa
--tension	483 MPa
MODULUS OF ELASTICIY	28.3 GPa

4.4.2 Resin

Selection of the resin was determined by storagability, flexibility, stickiness, ability to cure, and ability to withstand space conditions. Resin H (LMB 2804/2805) was the resin material to be chosen. Resin D was not chosen because its reactivity was not as high as resin H's and its storagability was not as good as resin H's. Resin E was more reactive than resin H, but after being stored for a period of time it became tacky. Resin G's reactivity was not as high as Resin H's [Reference 9].

Thus, resin H was chosen to be the resin for the

composite for the following reasons [Reference 9]:

1. Better storage stability.
2. Better bond strength of prepregs.
3. Higher Stiffness.
4. Better thermal aging stability after cure.

The material properties of resin H (LMB 2804/2805) are shown in Table 4.5.

Table 4.5. LMB 2804 - Resin Matrix Properties

BENDING STIFFNESS	3.3 MPa
TEAR STRENGTH	8.7 kN/m
TENSILE STIFFNESS	342 kN/m
MIXING RATIO OF LMB 2804:LMB 2805	100:15
MODULUS OF ELASTICITY	3.4 GPa
ELONGATION	5 %

4.4.3 Composite

Figure 4.2 shows the Kevlar/LMB 2804 composite temperature ranges versus tensile strength. For the temperature ranges that this satellite will experience this graph shows no degradation due to space conditions. The curing time for rigidization of this satellite is 3 hours at 120 °C. Figure 4.2 also shows that this temperature is within the composite's ranges of temperatures in which no degradation will occur within the time to cure [Reference 11]. Table 4.6 lists the material properties of the composite, which has a thickness of 700 micrometers.

Table 4.6. Composite (Kevlar/Resin) Properties

DENSITY	1.38 g/cm3
TENSILE STRENGTH	
0° direction	1380 MPa
90° direction	27.6 MPa
COMPRESSIVE STRENGTH	
0° direction	276 MPa
90° direction	138 MPa
IN-PLANE SHEAR STRENGT H	44.1 MPa
INTERLAMINAR SHEAR STRENGTH	48 - 69 MPa
POISSON'S RATIO	0.34
TENSILE/COMPRESSIVE MODULUS	
0° direction	75800MPa
90° direction	5500MPa
IN-PLANE SHEAR MODULUS	2070 MPa

The composite material is used to cover the antennas and the toroid. The placement of the materials for the antennas can be seen in Figure 4.3, while the placement of the materials for the toroid is depicted in Figure 4.4.

4.4.4 Other Materials

Kapton film is a polyimide and serves as a gas barrier for the satellite. The Kapton film properties are listed in Table 4.7, and it has a thickness of 13 micrometers.

Table 4.7. Kapton Properties

ULTIMATE ELONGATION	68 %
TENSILE STRENGTH	31290 lb/sq in
TENSILE MODULUS	4694000 lb/sq in
TEAR STRENGTH	340 g/mm
DIELECTRIC STRENGTH	6.7 KV
VOLUME RESISTIVITY	1 E17 ohm cm
WATER ABSORPTION	2.1 %
SHRINKAGE	2.5 %

The metallic aluminum is the material that covers the reflective side of the antenna, but it has no use for the toroid. The properties of the metallic aluminum are not

listed because the metallic aluminum coating is very thin, only 60 nanometers, and therefore its properties are negligible as compared to the properties of the Kapton film. The polyurethane bladder is the material that gives the torus of the antenna its shape. This bladder is then covered by a polyester cloth that is reinforced radially by Kevlar 49. LMB 2805 is a gaseous catalyst for curing. In other words, it is the material that interacts with the curing gas and rigidizes the satellite, where boron triflouride, BF_3, is the curing gas [Reference 9].

4.4.5 Surface Coatings

Indium tin oxide and metallic aluminum are the materials chosen as the surface coatings to protect the satellite from the space environment. Indium tin oxide (also with a thickness of 60 nanometers) is the material that covers the toroid and the radome side of the reflector, while the metallic aluminum covers the reflective side of the antenna. Both coatings can prevent the penetration of ultraviolet radiation, and both can also resist impact from micrometeorites. Furthermore, both can provide good thermal protection for the spacecraft, plus the phenomenon of spacecraft charging can be greatly reduced.

4.5 Materials Costs

The costs and weights of the various materials were found through various companies. They are specified in the

following table (Table 4.8):

Table 4.8 Material Costs

Dupont:			
Kevlar Fiber	weight	1420 g / 9000 meters	
	cost	$20 / lb	[Reference 11]
Burlington Glass Fabrics:			
Kevlar Cloth	weight	5 oz / sq yd	
	cost	$9.28 / sq yd	[Reference 6]
American Cyanamid:			
Composite	weight	240 g / sq m	
	cost	$18.85 / linear yd	[Reference 3]
Sierracin:			
Kapton with:			
Metallic Aluminum	weight	18 g / sq m	
	cost	$6 / sq ft	
Indium Tin Oxide	weight	18 g / sq m	
	cost	$6 / sq ft	[Reference 24]

The composite is to be made of two laminates of unidirectional Kevlar fibers imbedded into the LMB 2804 resin oriented at a 45 degree angle to each other. Originally, the composite material was to be made of a Kevlar cloth imbedded in the LMB 2804 resin. This changed, however, because of cost, for it is much cheaper to impregnate unidirectional fibers in the LMB 2804 resin than it is to impregnate the Kevlar Cloth in the LMB 2804 resin. The Kevlar fiber makes up 2/3 the cost of the composite, while the resin makes up 1/3 the cost of the composite.

ORIGINAL PAGE IS
OF POOR QUALITY

Figure 4.1

STRESS VS. STRAIN

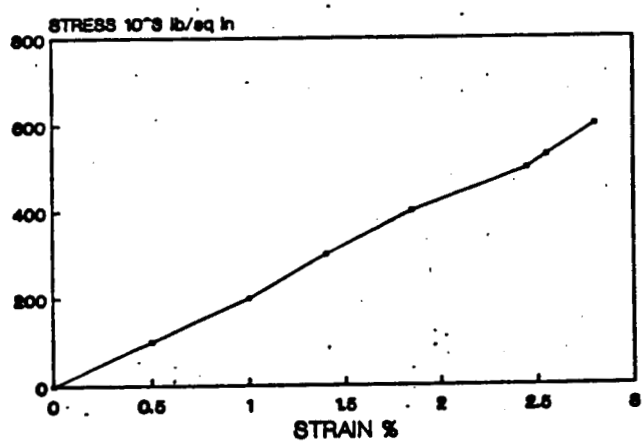

Figure 4.2

TENSILE STRENGTH VS. TIME

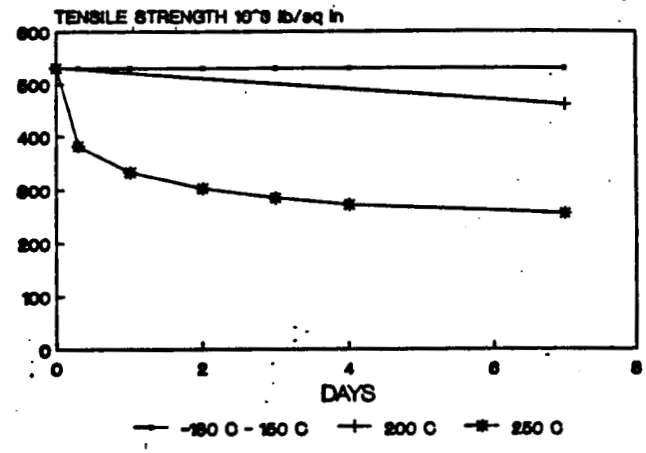

Figure 4.3

ANTENNA MATERIAL POSITION

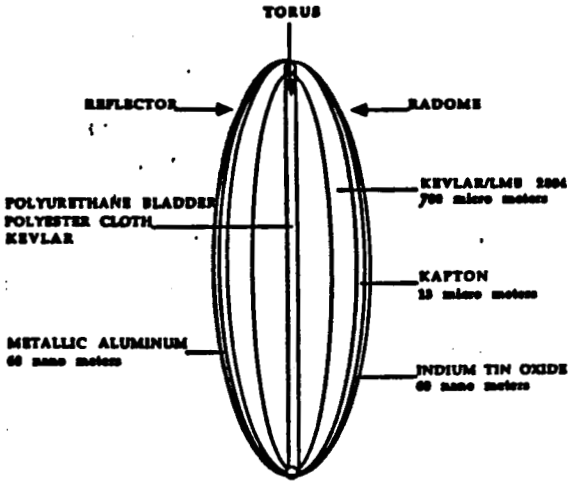

Figure 4.4

TOROID MATERIAL POSITION

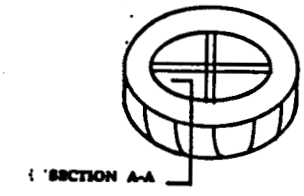

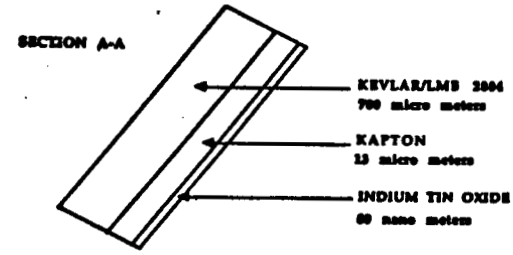

5.0 HEAT TRANSFER

Once the materials are chosen, it is necessary to verify that they can, indeed, hold up under space conditions. Thus, it is necessary to perform a heat transfer analysis.

5.1 Conduction

In a spacecraft, heat is mostly transferred by conduction throughout the solid parts of the spacecraft and radiated across the interior volume and into space from the external surfaces [Reference 1]. For the conduction analysis, the heat is transferred from the interior to the exterior by going through several different layers of materials: the composite, kapton, and selected coating, oriented in this order. Since the composite is the thickest (700 micrometers) among all three, and the other two are relatively much thinner (kapton and coating = 60 nanometers), their presence will be ignored in the analysis. In other words, the rate of heat conduction will be analyzed as if it were passing through one wall (composite), instead of passing all three layers. However, from the resources received, there is no thermal conductivity for the composite. Thus, there is no conduction through the material.

5.2 Radiation

Radiation is another mode of heat transfer the

spacecraft will encounter. When radiation falls on a body, a fraction of it is absorbed (α), a fraction is reflected (ρ), and the remainder is transmitted through the body (τ). These fractions are related by:

$$\alpha + \rho + \tau = 1 \qquad (5.1)$$

In the analysis of radiative heat transfer, it is useful to introduce the concept of blackbody. A blackbody can absorb all radiation incident upon it, and thus ρ and $\tau = 0$. Furthermore, it emits, at any particular temperature, the maximum possible amount of thermal radiation [Reference 1]. The rate at which energy is radiated from a blackbody is proportional to the fourth power of its absolute temperature [Reference 7]:

$$E_b = (\sigma) * T^4 \qquad (5.2)$$

where:

E_b = rate at which energy is radiated from a unit area of surface of a blackbody to the hemisphere of space above it (W/m^2)
σ = Stefan - Boltzmann constant
T = absolute temperature

At a maximum equilibrium temperature of 150 °C (323 K):

$$E_b = 2.398 \text{ E-5 } W/m^2$$

5.3 Intensity of Radiation

The intensity of radiation is assumed to be in a direction normal to the emitting surface.

Then:

$$I = E_b / \pi \qquad (5.3)$$

$$I = (2.398\ E\text{-}5)/3.14$$

$$I = 7.633\ E\text{-}6\ W/m^2$$

5.4 Kirchoff's Law

Kirchoff's Law states that, at a given wavelength, the absorptivity and emissivity are equal. Thus:

$$\alpha = \epsilon \qquad (5.4)$$

However, realistically α and ϵ are a function of the wavelength. Therefore, in practice, α and ϵ are different in most cases.

5.5 Calculation of Coating Property (α/ϵ) vs. Temperature

Spacecraft temperatures are computed from solutions of simple heat balance equations :

heat stored = heat in - heat out + heat dissipated (5.5)

where

heat in = absorbed sunlight, reflected sunlight (albedo), planet emitted radiation

heat out = infrared radiation from external surface

heat dissipated = electrical and electronic components

For simplicity, and convenience, the assumptions for the spacecraft are:

(1) infinitely conductive
(2) isothermal
(3) spherically shaped
(4) earth's radiation is negligible
(5) no dissipative equipment

Then

$$\text{heat out} = \text{heat in} \qquad (5.6)$$

$$(\epsilon)(\pi)(R^2)(\sigma)(T^4) = (\alpha)(S)(\pi)(R^2) \qquad (5.7)$$

$$T = \{(\alpha/\epsilon)(S/4\sigma)\}^{1/4} \qquad (5.8)$$

where

σ = Stefan - Boltzmann constant --- 5.67E-8 $W/m^2\text{-}K^4$
ϵ = emissivity
α = absorptivity
S = solar flux

Table 5.1 depicts equation 5.8 for S = 1353 W/m^2 (Yearly average value) :

Table 5.1 α/ϵ vs. T for S = average value

α/ϵ	T (K)
.01	87.89
.10	156.28
.25	196.52
.45	227.62
.70	254.21
.90	270.69
1.0	277.92
3.0	365.76
4.0	393.03
5.0	415.58
6.0	434.96

For S = 1400 W/m^2 (Maximum - perihelion of earth's orbit) :

Table 5.2 α/ϵ vs. T for S = maximum value

α/ϵ	T (K)
.01	88.64
.10	157.62
1.0	280.3
2.0	333.33
3.0	368.9

Table 5.3 depicts equation 5.8 for S = 1309 W/m^2 (Minimum - aphelion) :

Table 5.3 α/ϵ vs. T for S = minimum value

α/ϵ	T(K)
.01	87.16
.10	155
1.0	275.6
2.0	327.78
3.0	362.75

According to Figure 3.3, the ratio of absorptivity and emissivity of the surface coating must lie within the range of .05 to 1.3. (Notice that the value of the solar flux used in Figure 3.3 is the yearly average value of the solar flux in the geostationary orbit.) The coating which will be used for this large antenna array does just that. These parameters were computed for various parts of the spacecraft, and the results are as follows:

Antenna reflector: $\alpha=0.2$, $\epsilon=0.9$

Solar panel and antenna: $\alpha=0.84$, $\epsilon=0.85$

Solar cells: $\alpha=0.65$, $\epsilon=0.82$

6.0 PROPULSIONS

There are two types of propulsion systems that need to considered for the satellite. The first is to boost the satellite to geosynchronous orbit after it has been cured. The second is for attitude control while it is in orbit.

6.1 Orbital Transfer

The placing of ISAAC into geosychonous orbit from low earth orbit will involve the use of the orbit transfer vehicle (OTV) with the transfer orbit stage (TOS) [Reference 27]. The all propulsive OTV can boost 7,600 kg in geosychonous orbit. However, the aero-assisted OTV, which saves 35% of the propellent by using the Earth's atmosphere to break on the return to the space station, can boost 10,720 kg [Reference 28]. Thus, the aero-assisted OTV will be utilized. Since the weight of ISAAC is 15,348 kg, the aero OTV needs to be assisted by the TOS. The TOS can boost 6,000 kg into geosychonous orbit and is designed for other booster stages. With a modified attachment, the TOS can work with the OTV giving a total payload capability of 16,000 kg.

6.2 Attitude Control System

The attitude control system requirements necessary on the antenna system include: orbital correction, stabilization, and repositioning of the array. Key design

factors include: reliability, low mass, low cost, and long duration. Due to the very large diameter of the torus and relatively small mass, the thrust force required for repositioning is very small. For these reasons it was decided to go with a derivative of the space shuttle's vernier propulsion system. This system has a proven track record in space operations, and having been already manufactured would prove to be a more cost effective alternative than a complete redesign of the entire propulsive system. Each thrust chamber has a mass of only 3.18 kg, and the thrusters have been fired over 300,000 times over a total of more than 23 hours without a failure.

6.2.1 Thrust Chamber Characteristics

The thrust chamber is pictured in Figure 6.1 with all appropriate dimensions labeled. The thruster uses monomethylhydrazine (MMH) for fuel and nitrogen tetroxide (N_2O_4) for its oxidizer at a mass mixture ratio of two parts oxidizer to one part fuel. Although the gas exiting from the thrust chamber is highly toxic, the location of the array in geostationary orbit, far from man, makes this factor unimportant. The pressure in the supply tanks are each kept at 1.70 MPa. The thrust chamber is capable of supplying 111.2 Newtons of thrust and a specific impulse of 260 seconds with a thrust chamber pressure of 760 MPa. The propellant flow rate through the thruster is 0.0281 kg/sec.

6.2.2 Propellant Mass and Storage

The system will be designed to carry enough fuel for one hour of continuous operation. With the above given propellant flow rate, the mass of the oxidizer and fuel can be calculated to be 101.2 kg. From this and knowledge of the mixture ratio, it is calculated that the mass of the MMH required will be 33.73 kg, and the mass of the N_2O_4 will be 67.47 kg.

6.2.3 Fuel Tank Sizing

The fuel tank must carry 33.73 kg of MMH at a pressure of 1.70 MPa. The specific gravity of the MMH fuel is 0.8788 at 293 degrees Kelvin. This means the density of the liquid fuel is 878.8 kg/m^3. The required tank volume can be computed to be 0.03838 m^3. Addition of 5 percent for extra fuel and ullage brings the total tank size up to 0.04032 m^3. The tank will be cylindrical in shape with a radius of 0.15 meters, which means that the overall length of the tank will be 0.671 meters.

6.2.4 Oxidation Tank Sizing

The oxidation tank carries 67.47 kg of nitrogen tetroxide which has a density of 1447 kg/m^3 at 293 degrees Kelvin. The result is a required tank volume of 0.04898 m^3, again with the 5 percent ullage and excess oxidizer added in. Staying with a cylindrical shape of the same radius as the fuel tank of 0.15 meters, this yields an overall tank length of 0.793 meters.

6.2.5 Pressurization Tank Sizing and Initial Gas Mass

The pressurization tank sizing depends on the mass of the gas present in the tank and the pressure and temperature that the gas is stored at. The mass of the gas in turn depends upon the pressure and the volume of propellant that it must act upon. A simplified analysis for preliminary design was used [Reference 25] which makes use of the relation:

$$M_o = P_p(V_p)(k)/[R(t_o)(1-P_p/P_o)] \qquad (6.1)$$

Where

M_o = Initial mass of gas to expel all propellants

P_p = Pressure in propellant tanks

V_p = Volume of both propellant tanks

k = Specific heat ratio of the gas

R = Gas constant for the gas

T_o = Initial storage temperature of the gas

P_o = Initial gas storage pressure

Evaluation of the above relation using air (R = 230 J/kg K; T_o = 293 K; k = 1.40) as the pressurizing gas, with initial gas pressure of 10.0 MPa, propellant pressure of 1.70 MPa, and propellant tank volume of 0.08926 cubic meters results in a initial gas mass of M_o = 0.004 kg. The pressurization tank volume is then determined to be V_o = 0.02561 cubic meters. Once again using a cylindrical tank with a radius of 0.15 meters, the tank length will then be determined to be 0.463 meters.

The assumptions made by using this equation are that the initial storage temperature of the gas is maintained, which in the case of an attitude control system is valid, as the expansion occurs slowly and it is therefore nearly an isothermal process. Additionally, it is assumed that the temperature it is inflated at is the temperature of the surrounding medium in which it is stored. Also assumed is that there is no heat transfer to the walls of the tank by the gas, or, in other words, that the process is adiabatic. The mass of the gas initially in the piping and propellant tanks is neglected, which in such a small system is an acceptable assumption.

The gas used as the pressurant was chosen to be air [Reference 25] because it is readily available and inexpensive. Because the craft does not spin, an elastic diaphragm will have to be used in both the oxide and fuel tanks as a positive expulsion device. This will keep the propellants from leaving the tank outlet and floating or mixing with the pressurized gas. In the case of the monomethylhydrazine, which is known to react with air, the diaphragm will also serve as a protective barrier between the chemically active gas and the fuel.

6.2.6 Tank Construction

Due to the reactivity of the MMH with many common types of materials, the composition of the fuel tank is limited to a few different materials. Listed below, in Table 6.1, is a trade off study using three different materials which would

not react with the MMH fuel.

Table 6.1 Material Trade Off Study

Material	Density kg/m^3	Max Stress* MPa	Thickness cm	Mass kg
Stainless Steel 304	8020	308.9	0.083	4.17
Aluminum Alloy 3003	2730	110.3	0.231	4.03
Nickel Astm B160	8890	331.0	0.049	4.34

* The maximum stress was computed having known the value of the elastic modulus and then assuming a standard strain of 0.002, the result was then divided by a safety factor of 1.25.

Based on this comparison study the aluminum alloy was chosen for the construction of the tank. At the time of this writing the price of the different materials was unavailable for comparison. If one of the other materials offered a significant cost savings over the aluminum then it would be easy enough to switch materials without drastically increasing the weight. It was decided for preliminary analysis to make the oxidation and pressurization tanks out of the same material. This results in the oxidation tank having a mass of 4.76 kg, and the pressurization tank having a mass of 2.77 kg.

6.2.7 Thrust Module

The basic thrust module is pictured in Figure 6.2 and shows the overall layout of each thrust control module. There are five thrust chambers on each module which share a single propellant, oxidation, and pressurization tank. The location of the thrust chambers was designed to keep as much of the chamber inside of the module as possible to make for a tighter and more efficient fit into the space shuttle's cargo bay.

The pressure regulator on the top of the pressurization tank functions to keep the pressure in the fuel and the oxidation tanks at a constant pressure of 1.70 MPa. Two lines from each tank run to their own five way valves used to send propellant to the desired thruster. One line is a primary line and the other is a secondary line. The primary line is for normal use, and the secondary line, built for redundancy, is used in the event of failure of the primary line. The secondary line could also be used in the event that it was necessary to fire more than one thruster on a module at the same time. The five way valves are controlled by a computer at the center of the torus, which receives sensor information and computes which thrusters should be fired for what amount of time in order to adjust the position of the antenna array.

The mass of the entire module is summarized below in Table 6.2:

Table 6.2 Thrust Module Mass

Thrust Chambers (5)	15.90 kg
Fuel and Tank	33.73 kg
Oxidizer and Tank	72.23 kg
Pressurization Gas & Tank	2.81 kg
Hoses, Regulators, & Valves	2.50 kg
Supports	3.50 kg
Total	134.67 kg

6.2.8 Total System Integration

The system will contain four thrust modules, each one located at the intersection of the cross members and the circumference of the torus. This will allow for twenty independent thrust chambers, with the total mass of the attitude control system totaling 538.68 kg. Because each module contains enough fuel for 3,600 seconds of operation, the total operating life of the attitude control system will be 14,400 seconds (4 hours). As a result of the symmetrical location of the modules, the chambers can be used in tandem, for example, a thruster on one side fires up and the thruster on the other side of the antenna fires down. The RIS cloth will be manufactured into the thrust modules and the entire package will be pre-assembled on Earth, which will make deployment easier as no in space joining of the structure will be necessary. The electrical wires going to the central control computer will be run inside the cross members, which will keep them protected from the space environment.

Figure 6.1

Attitude Control Thrust Chamber

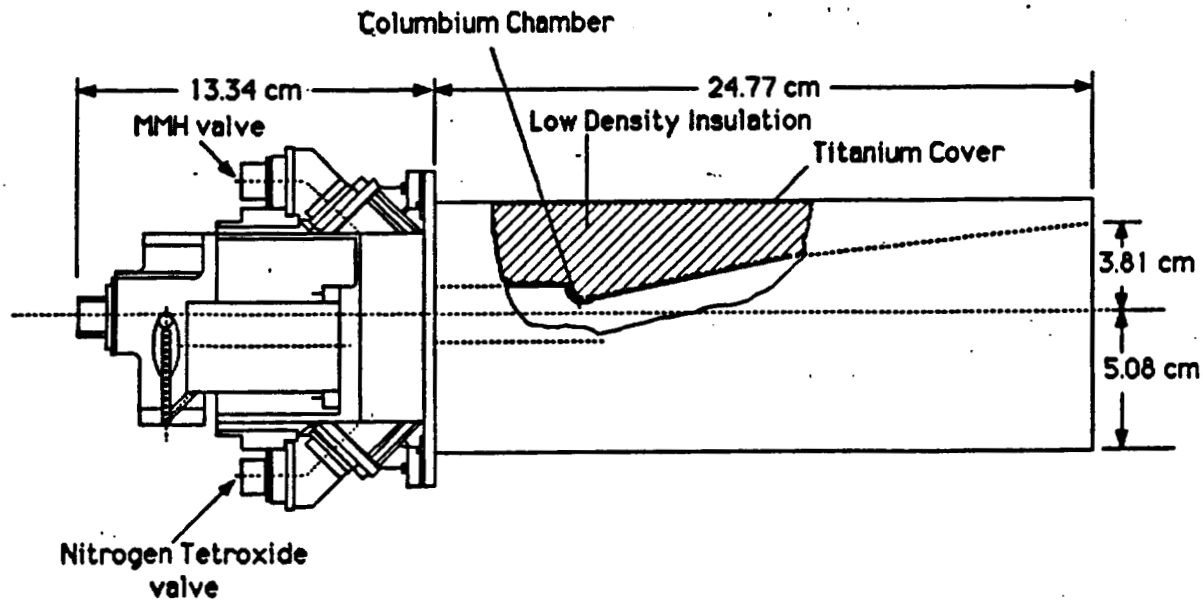

Figure 6.2

Attitude Control Propulsion Modual

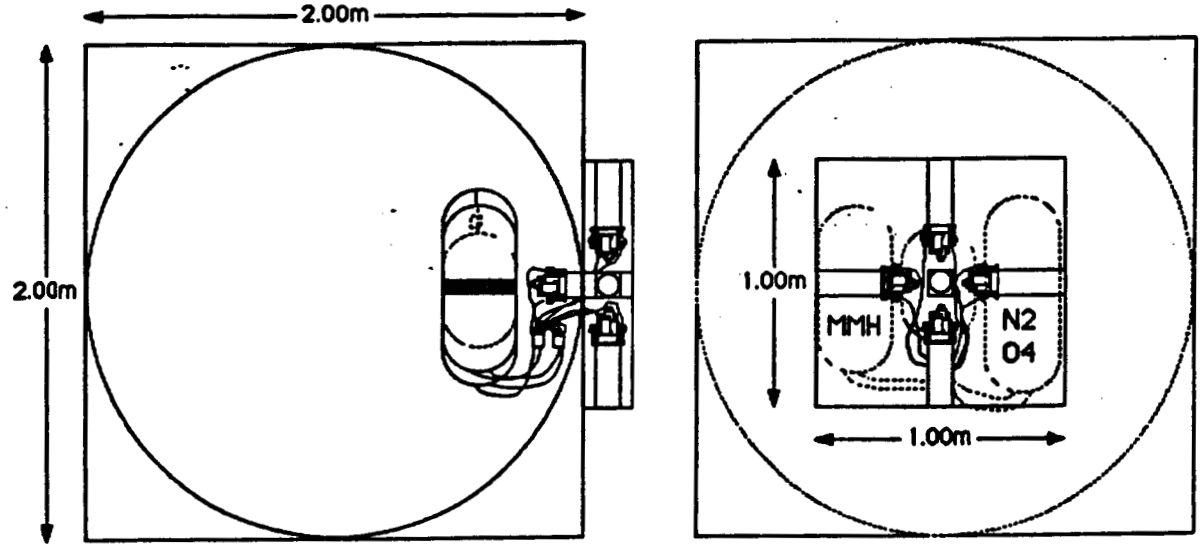

7.0 STRUCTURAL ANALYSIS

A static analysis was performed to determine the structural integrity of the antenna support system. The analysis included the torus and cross members of the satellite, and focused on the rigidized structure (after inflation and curing at the space station). An initial size for the cylindrical cross-sections of the torus and cross members was based on a bending stress analysis. Critical loads were determined for the satellite's orbit, and were used for the analysis. The structural analysis was performed using finite element methods, utilizing an expanded version of the NASA Structural Analysis code, MSC Version 65 (NASTRAN). Preprocessing and postprocessing of the finite element model were performed with the aid of the PATRAN code.

7.1 Initial Structural Sizing

The radius of the torus structure itself had been determined based on the space that would be necessary to accommodate the 24 antenna subassemblies. This radius was found to be 75 meters, and allowed enough room to account for any interference effects.

The next step in sizing the torus and cross-members was to determine the radii of their tubular cross-sections and their wall thicknesses. It was decided to keep the radius of the torus cross-section equal to that of the cross-members to

allow all of the mounts for the antenna subassemblies to be the same size. This would also make production of the subassembly mounts and of the torus and cross-members more cost efficient, by eliminating any extra tooling that might be required. However, since the cross-members should require a smaller cross-section due to their smaller loading in comparison to the torus, keeping the radius of the cross-members equal to that of the torus does add extra weight to the structure. The lower limit for the tubular cross-section radius was approximated from an initial sizing of the subassembly mounts, and was found to be .35 meter.

It was necessary to find a relationship between the radius and thickness of any cross-section. It was decided to equate these two parameters through the elastic flexure formula for normal stress [Reference 17], since the allowable stress limits had been defined by the material selection (refer to Section 7.3.6 Physical Properties). An analysis of a cylindrical cross-section with respect to the maximum bending moment expression determined the equation of the maximum bending or normal stress to be:

$$\sigma = 1.5Pr/\pi t^2 b \qquad (7.1)$$

where

P = Vertical Shear Force

r = average cross-section radius

t = wall thickness

b = cross-section thickness (= 1 inch)

An expression for the total volume of the torus and

cross-members was determined to be as follows:

$$V_{tot} = 4845.8rt \quad (m^3) \qquad (7.2)$$

From the above equation and the fact that volume=mass/density, and using a density of 1380 kg/m^3, the following equation for the total mass of the torus and cross-members was determined:

$$m = 6.687 \times 10^6 \, r \, t \qquad (7.3)$$

An upper limit for the mass of the support structure was found to be approximately 5000 kg. This value was based upon a maximum launch load of approximately 14,000 kg and the distribution of the mass among the other satellite components, as follows:

+ Maximum Launch Mass	= 14000 kg
- Solar Array Mass	= 250 kg
- Total Reflector Mass	= 8448 kg
- Controls (approx.) Mass	= 200 kg
- Miscellaneous Mass	= 100 kg
Total for Support Structure	= 5000 kg

Various plots were made utilizing the equation for maximum bending stress (equation 1) to identify trends in the variables r, t, and σ. Since an accurate load distribution was not available, it was decided to assume a unit load for the vertical shear load, P, which would still show the general trends. Figure 7.1 is a plot of wall thickness

versus the cylindrical radius using equation 7.1, and letting the stress be equal to the yield stress (704 MPa). This graph shows that, for a constant stress, as the radius increases the thickness must also increase. Therefore, it is desirable to keep the radius small to keep the volume and mass small. Figure 7.2 is a plot of stress versus cylindrical radius, again using equation 7.1. This graph was plotted with the conditions of a unit load and unit thickness, and shows that the stress increases linearly with increasing radius. Figure 7.3 is a plot of stress versus thickness, using equation 7.1 for a constant radius (unit radius) and unit load. This figure shows that the stress decreases with increasing wall thickness. A comparison of Figures 7.1 and 7.3 shows that the wall thickness provides the major influence with respect to stress.

Since the thickness was the major contributor to the reduction in stress, it was decided to choose an approximate value for the radius and vary the thickness during the actual structural analysis. The lower limit for the radius (.35 meter), which was sited earlier, was judged to be too small to handle the loading. An approximate radius of 1 meter was chosen on the basis of the reflector subassembly mount. Too large a radius would require a larger mounting assembly and add further weight to the overall structure.

The minimum skin thickness was chosen on the basis of the allowable stress. To simplify the calculations, an average stress was vectorally determined based on the maximum

tensile stresses in the fiber and matrix directions, and was found to be 703.8 MPa. Based on this allowable stress and the equation for maximum bending stress, the minimum thickness was determined to be 26 micrometers. Allowing for the fact that a unit load was assumed, the minimum thickness was increased to 100 micrometers. This number would later be found to be much too small (refer to Section 7.4 Results).

The maximum thickness was determined from the maximum allowable mass for the support structure (approximately 5000 kg). Using the equation for the total mass, which is related above, the maximum skin thickness was found to be 748 micrometers.

7.2 Orbital Mechanics

The acceleration of the satellite can be determined from:

$$a = R - \Omega \times (\Omega \times R) - \Omega \times (\Omega \times r) - 2\Omega \times V \qquad (7.4)$$

where

R is the acceleration due to gravity

$\Omega \times (\Omega \times R)$ is the centrifugal acceleration due to the moving reference frame

$\Omega \times (\Omega \times r)$ is the centrifugal acceleration due to the satellite

$2\Omega \times V$ is the coriolis acceleration

Since $\Omega = .728 \times 10^{-4}$ rad/s, the two centrifugal acceleration terms are negligible compared to the coriolis term for low altitude orbits. The gravitational acceleration

changes with the altitude at which the satellite orbits the earth; it is inversely proportional to the inverse square of the altitude.

To determine the velocity at which the satellite orbits the earth, orbital mechanics were applied. Hohmann Transfer is utilized with the assumption that the transfer occurs between the two circular concentric orbits. Figure 7.4 shows the path of the satellite transfer from space station orbit to geostationary orbit.

From equation 7.4, the acceleration was determined to be 8.505 m/s^2 at the space station and .500 m/s^2 when it reaches geostationary orbit. This result appears to be correct due to the fact that the dominant term in the acceleration equation is the gravitational term. Since the space station orbits above the earth at 500 km and the geostationary orbit is at an altitude of 35,860 km, one would expect the acceleration to be much greater at the space station [Reference 20].

7.3 Finite Element Analysis

The finite element analysis was performed through the use of MSC/NASTRAN, Version 65, and the PATRAN pre- post-processing software. The analysis was carried out for two loading situations: one for the loads encountered at the initial boost from space station orbit, and one for loads encountered during the satellite's final geostationary orbit.

The main objective of the analysis was to determine the amount of out-of-plane warping the torus would exhibit during the critical loading stages. It was also desired to determine the stress/strains over the entire structure, focusing on the intersections of the torus and cross-members.

7.3.1 Finite Element Theory

The finite element theory is based upon the following concepts: subdivision and continuity [Reference 29]. The concept of subdivision is simply that space is finite and infinitely divisible. The concept of continuity is that a continuous quantity is made up of infinitely divisible elements. These two concepts allow for the division of objects into smaller units, or Finite Elements.

The finite element method involves the following steps:

1) Discretization - division of the object into finite elements.

2) Selection of the Interpolation Function - usually a polynomial is used to specify the field variable over the element. The number of coefficients in the polynomial equals the number of degrees of freedom.

3) Determination of the local element characteristics - determination of the stiffness matrix and nodal force vector in terms of the element coordinate system.

4) Transformation of the Element Characteristics - change from local (element) coordinate system to the global coordinate system.

5) Assemblage of the Global Element Characteristics

6) Application of the Boundary Conditions

7) Interpretation of the Results

7.3.2 NASTRAN: The Input

Computations for the static analysis of the torus and cross members were done using the finite element code of NASTRAN, Version 65. The NASTRAN code is capable of performing many different types of analyses, including static and dynamic structural analysis, heat transfer analysis, and fluid dynamics analysis. Solution 24, which is a rigid format statics analysis in the NASTRAN code, was utilized to perform the calculations. Isoparametric membrane-bending quadrilateral (QUAD4) and triangular (TRIA3) plate elements were used to model the structure. Plate elements were chosen because the structure is basically that of a hollow balloon. These elements are plane stress/strain elements. Since these elements are isoparametric, the displacement functions are of the same order as the lines connecting the nodes. This gives more accurate results for the curved surfaces of the structure. NASTRAN QUAD4 elements are capable of handling layered composite materials, via the PCOMP property card and the MAT8 material card. A seven ply lay-up was used to model the KEVLAR composite. Loads were input to NASTRAN through the GRAVITY, FORCE, and LOAD cards.

7.3.3 NASTRAN: The Output

The results of the static analysis included displacements, forces, stresses and strains. Nodal displacement vectors are calculated with reference to the global coordinate system by the NASTRAN code. Nodal displacements are found in the x, y, z directions, as well

as for rotations about each of the axes. The number of grid point (nodal) rotations is limited when using two-dimensional elements. This will be discussed further in Section 7.3.5.1 Constraints.

NASTRAN is capable of outputting many different types of force data. In this case, forces of the single point constraints, forces in the quadrilateral elements, and grid point force balances were requested as output. The single point constraint forces occur only at those grid points which have been specifically requested to be restrained in a certain direction or rotation. The single point constraint forces are reactionary forces and moments. Membrane forces, bending moments and transverse shear forces were calculated for the quadrilateral elements. Grid point force balances were found at the nodal points, and are calculated in the x, y, and z directions and for rotation about the three axes.

Stress output was determined for the stresses in the layered composite quadrilateral elements. NASTRAN has the capability of analyzing the stresses in the various plys of a composite material (refer to Section 7.3.5.2 Composite Modeling). Therefore, stresses are calculated for each ply in the lay-up. Normal and shear stresses are found in the fiber and matrix directions. Inter-laminar shear stresses and principal stresses were also calculated. All stresses are calculated with reference to the element (local) coordinate system.

Failure criteria were also outputted through the NASTRAN

code. These results include failure indices for the layered composite elements. The Hoffman failure theory was used to calculate the failure indices for each ply. The failure indices included those for direct stresses, inter-laminar stresses, and a maximum index for all piles of any individual element.

Strains were outputted for each of the quadrilateral elements. Strains are calculated with reference to the element coordinate system. Normal-X, Normal-Y, and Shear-XY strains were calculated. Also, the principal strains and Von Mises strains were found.

7.3.4 Preprocessing and Postprocessing

The physical finite element model was preprocessed using the PATRAN code. This same code was also used to view the results of the finite element analysis. PATRAN is a code which can be interfaced to and from the NASTRAN code.

7.3.4.1 PATRAN: Preprocessing

The physical model was constructed using PATRAN and then input (interfaced) to the NASTRAN code. This method of physical modeling is very useful in that each node or element does not need to be manually input to NASTRAN. The PATRAN code allows the user to discretize the structure with the desired number of elements. It also allows for easy changes to the model, without the necessity of tedious hand calculations.

7.3.4.2 PATRAN: Postprocessing

The results of the NASTRAN finite element analysis were visualized with the aid of PATRAN postprocessing techniques. NASTRAN results are translated back into PATRAN, and the various types of output can be plotted on the finite element model. The physical deformation of the structure was plotted. PATRAN is also capable of plotting stress/strain distributions throughout the structure in the form of topological contours plots of the various stress/strain intensities. Plots of the grid point forces were also done with PATRAN.

7.3.5 The Model

It was desired to make the finite element model as simple as possible without having a significant amount of inaccuracy. The complete support structure, with full torus and cross-members would require a large number of nodes and elements (approximately 840 elements). To avoid such a large number of elements, the structure's symmetry was utilized. The structure contains symmetry about two of its planes. Therefore, only one-quarter of the structure need be analyzed. Figure 7.5 shows the finite element model and the chosen coordinate system.

The model contained a considerable amount of nodes and elements. Two-hundred and fifteen nodes and two-hundred and six elements were used. The circular cross-sections of the torus and cross-members were divided into eight equal sections. The circumference of the torus was divided into 16

equal sections. Two of these sections, at the intersections of the torus and cross members, were further subdivided into five smaller sections to obtain more accurate results at these intersections. The cross members were each divided into five sections.

The intersections of the torus and cross-members were to some extent filleted to ease out some of the stress at these intersections. The intersection of the two cross-members was not filleted. This was to allow for a specific set of constraints to placed at this intersection. The same model was used for both cases of loading.

7.3.5.1 Model Constraints

Since the model was quartered along its two planes of symmetry, it was necessary to constrain the edges along these planes from any lateral motion (into the planes). The upper edges of the halved cross-members were also restricted from motion in the vertical direction, but were allowed to move horizontally or parallel to their respective planes of symmetry. The lower edges of the cross-members were allowed to move in the vertical direction due to the fact that the concentrated loads of the reflectors would be placed along these edges and act in the vertical direction, and they were also allowed to move horizontally parallel to their planes of symmetry. The model was constrained so that the one-quarter of the model was essentially held-up by the other three-quarters of the model.

All nodes in the model had to be restrained from all rotations. This was to eliminate any discontinuities along the boundaries of the elements, in terms of the rotational slopes.

7.3.5.2 Composite Modeling

Laminated composites are comprised of a series of individual lamina stacked one above another, with each laminae defined by a different orientation of the principal material directions. MSC/NASTRAN has the capability to model an entire stack of laminae with a single plate or shell element. This is accomplished by organizing the material properties of the stack in the matrices of elastic moduli for the element. These matrices are automatically calculated in MSC/NASTRAN from thickness, material properties, and the relative orientation of these properties for the individual lamina. One unique feature of this software is that the laminae does not necessarily have to be manufactured with the same material. With the PCOMP and MAT8 bulk data cards, the user has the ability to define a different material property for each laminae [Reference 19].

MSC/NASTRAN performs these calculations based on classical lamination theory which incorporates the following assumptions:

1. The laminate consists of perfectly bonded laminae.
2. The bonds are infinitesimally thin and nonshear-deformable. This means displacements are

continuous across laminae boundaries so that no lamina can slip relative to another.

3. Each of the lamina is in a state of plane stress. An additional aid to the user is provided through optional output of a failure index for individual laminae. If the failure index is less than one, the lamina stress is interior to the periphery of the failure surface and the lamina is assumed safe. Conversely, if the failure is greater than one, the lamina stress is exterior to the periphery of the failure surface and the lamina is assumed to have failed.

MSC/NASTRAN allows the user to analyze failure with the following theory: Hill's Theory, Hoffman's Theory, and the Tsai-Wu Theory. For the inflatable satellite structure, orthotropic materials under a general state of plane stress with unequal tensile and compressive strengths were utilized. Hoffman's Theory for failure analysis was applied because it is best suited for this material type.

7.3.6 Physical Properties

The material properties of the KEVLAR 49 prepreg have been stated in this report (refer to Table 4.4). This section will summarize the properties which were necessary to perform the finite element analysis.

The following table (Table 7.1) lists the material properties for the unidirectional composite lamina, where the

0 degree direction defines the fiber orientation and the 90 degree direction defines the matrix orientation:

Table 7.1 Material Properties for the Lamina

Density (kg/m^3) = 1.38

Tensile & Compressive Modulus, 0 deg, (MPa) = 75800

Tensile & Compressive Modulus, 90 deg, (MPa) = 5500

Poisson's Ratio = .34

In-plane Shear Modulus, (MPa) = 2070

In-plane Shear Strength, (MPa) = 44.1

Interlaminar Shear Strength, (MPa) = 48-69

Allowable Tensile Stress, 0 deg, (MPa) = 1380

Allowable Compressive Stress, 0 deg, (MPa) = 276

Allowable Tensile Stress, 90 deg, (MPa) = 27.6

Allowable Compressive Stress, 90 deg, (MPa) = 138

7.3.7 Loading

Two separate loading situations were considered for the structural analysis. Case I considered the loads encountered during the escape from space station orbit to geostationary orbit. Case II considered the loads encountered during geostationary orbit.

The loads applied to the structure were limited to inertial and gravitational loads. The inertial loads were calculated from Newton's Second Law, F=ma. The critical acceleration (at boost from space station orbit) of 8.505 m/s^2, found from the orbital mechanics analysis, was used to

calculate the inertial loads for Case I. The acceleration at geostationary, .500 m/s^2, was used to calculate loads for Case II.

The inertia forces of the reflector subassemblies were converted to concentrated loads and were applied to the surface of the torus and cross members. Loads from the reflector subassemblies essentially pulled on the surface of the torus and cross-members in a vertical direction.

Gravity loads were considered for the torus and its cross members. However, loads produced by the attitude control boosters and the solar array tracking mechanisms were not considered. These loads were not considered to simplify the analysis, and they were also considered small in comparison to inertial and gravitational forces.

7.4 Results

Results of the finite element analysis are provided for both of the loading situations considered. The results include displacements, forces, stresses and strains.

7.4.1 Case I Results

The reactions to loads occuring during the boost from the Space Station to GEO orbit were determined. It was found that the magnitudes of the displacements were highly dependent upon the wall thickness.

7.4.1.1 Displacements

The final wall thickness had not been determined at the start of the finite element analysis. As stated previously,

an initial thickness of 100 micrometers was assumed. After performing an initial run of the NASTRAN code, it was determined that the resulting displacements were much too large and may damage the reflectors due to possibility of the reflectors colliding with one another. It was decided that the deflections should be five meters or less to keep the out of plane warping angle within five degrees. This would also assure that the stresses would remain in the elastic range and avoid plastic deformations. Several more iterations were necessary before determining the final thickness of 700 micrometers.

Using the thickness of 700 micrometers, displacements were found to range from -.0000494 to 4.97 meters. These values are in terms of resultant x, y, z deflections. The major deflections occurred in the vertical (y) direction as was expected due to the type of loads which were applied. Deflections along the cross-members were small, in the range of -.0000494 to .331 meters. Deflections along the torus ranged from .331 to 4.97 meters, with the maximum deflections occurring at the midpoint of the section torus. Figure 7.6 is a comparison of the non-deformed and deformed structure, while Figure 7.7 shows the magnitudes of the total displacement as a color coded magnitude distribution. Originally, all the outputs of PATRAN and NASTRAN were plotted in color as color coded magnitude distributions. Unfortunately, it was not possible to retain all the figures in color for this report.

7.4.1.2 Forces

Membrane forces in the quadrilateral elements ranged from 1.78 to 27500 Newtons. The largest of these forces occurred at the midpoint of the torus section. Bending moments for the elements ranged from .083 to 9.56 Newton-meters. Transverse shear forces ranged from .00099 to 36.0 Newtons.

Grid point force balances were calculated at each node in the structure. These balances represent the total force at each node resulting from the connecting elements, applied loads, and reactionary forces. A sample of this output has been provided in Appendix A.

7.4.1.3 Stresses

Normal and shear stresses were calculated in the fiber and matrix directions. The normal stresses ranged from approximately 2.0×10^{4} to 3.0×10^{7} Pascals. Shear stress ranged from approximately 1.0×10^{4} to 1.5×10^{7} Pascals.

Interlaminar shear stress was found to be from 3.0×10^{-4} to 2.5×10^{4} Pascals. Principal stresses ranged from approximately 1.1×10^{4} to 1.5×10^{7} Pascals. Maximum shear stress ranged from approximately 8.7×10^{4} to 2.2×10^{7} Pascals. All stresses were found to be lower than allowable limits.

Failure indices were all found to be much less than 1.0, showing that the composite material survived the applied loads.

7.4.1.4 Strains

Plots of strain contours were obtained through PATRAN postprocessing. All figures are color coded plots of strain magnitude distributions at the nodal points.

Figure 7.8 is a plot of the normal-x strains. These strains were found to be from -.00421 to .00308. The highest values were located near the intersections of the torus and cross-members on the upper surfaces.

Figure 7.9 is a plot of the normal-y strains. Values ranged from -.00239 to .00352. The largest values occurred on the lower surfaces near the torus/cross-member intersections.

Figure 7.10 is a plot of the shear-xy strains. These strains ranged from -.000558 to .000575. The distribution of the strains is complicated, and is best described by referring to Figure 7.10.

The distribution of the major principal strains is depicted in Figures 7.11 and 7.12. The strains ranged from .0000188 to .00353. The largest strains occur at the torus/cross-member intersections, and the lowest occur along the cross-members.

The strain distributions appear to be reasonable in magnitude and location.

7.4.2 Case II Results

The reactions to loads occuring during normal operations were also determined. Though the distributions are similar,

the magnitudes are much lower.

7.4.2.1 Displacements

The distribution of the resultant displacements is nearly identical to those of Case I (see Figure 7.13). The resultant magnitudes are much smaller for Case II and are between -.00000444 to .440 meters.

7.4.2.2 Forces

The force distributions for Case II are similar to those in Case I, but the magnitudes are much smaller. Membrane forces ranged from .085 to 2100 Newtons (approximately). Bending moments ranged from approximately 4.3×10^{-5} to .11 Newton-meters. Transverse shear forces were distributed between 1.02×10^{-5} and 5.0 Newtons.

7.4.2.3 Stresses

The stress distribution for Case II is similar to Case I with the exception of the magnitude. The magnitude of stresses are smaller than the first case. The normal stresses in fiber and matrix direction ranges from approximately 3.7×10^{3} to 2.7×10^{6} Pascal. The shear in the fiber and matrix direction is distributed from 2.0×10^{4} to 1.5×10^{6}. The interlaminar shear stress ranges from approximately 5.0×10^{-7} to 6.0×10^{3}. Principal stresses were determined to range from 9.0×10^{3} to 3.0×10^{6}. Maximum shears were found to be distributed from approximately 5.0×10^{4} to 1.2×10^{6}. These stresses also appear to be reasonable.

7.4.2.4 Strains

Normal-x strains were found to be from $-.375x10^{-3}$ to $.271x10^{-3}$. The highest values were located near the intersections of the torus and cross-members on the upper surfaces.

Values for the normal-y strains ranged from $-.21x10^{-3}$ to $.312x10^{-3}$. The largest values occurred on the lower surfaces near the torus/cross-member intersections.

Shear-xy strains ranged from $-.467x10^{-4}$ to $.502x10^{-4}$. Major principal strains ranged from .0000188 to .00353. The largest strains occur at the torus/cross-member intersections, and the lowest occur along the cross-members.

The strain distributions appear to be reasonable in magnitude and location.

7.5 Conclusions and Recommendations

1. The torus/cross-member support structure should be able to withstand the Case I loading condition of boost from space station orbit to geostationary orbit, without suffering plastic deformations. This is due to the fact that stress limits were well below elastic limits.

2. The largest deformations at geostationary orbit will result in a out-of-plane warping angle of approximately .336 degree. This will allow for sufficient accuracy in receipt or transmission of signals.

3. The structure should function without failure due to the fact that stress levels are well below the allowable limits.

4. It is recommended that the thickness of the cross-members be decreased to save on cost and volume. This would be allowable since the cross-members carry much less of the load.

Figure 7.1

THICKNESS VS. RADIUS

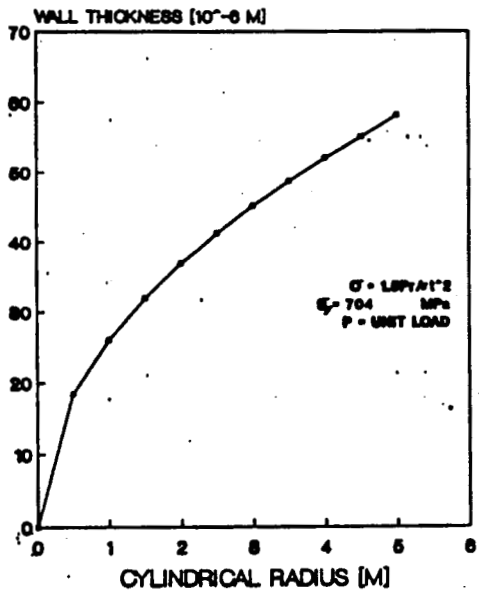

Figure 7.2

STRESS VS. RADIUS

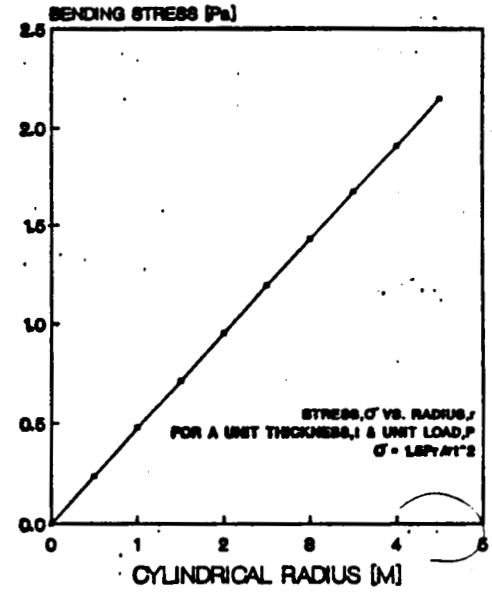

Figure 7.3

STRESS VS. THICKNESS

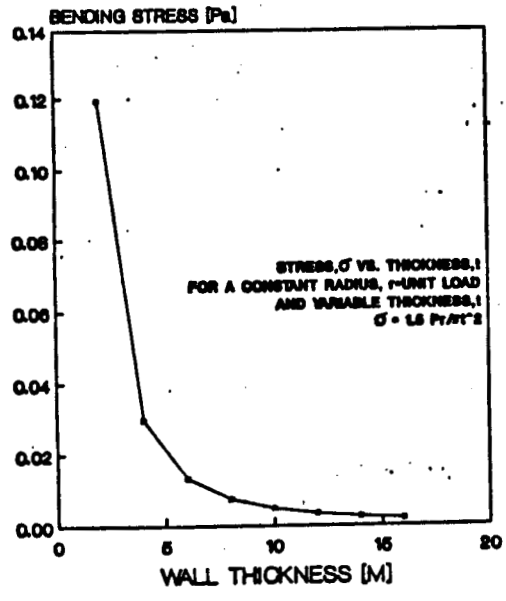

Figure 7.4

HOHMANN'S TRANSFER
FROM SPACE STATION ORBIT
TO GEO-STATIONARY ORBIT

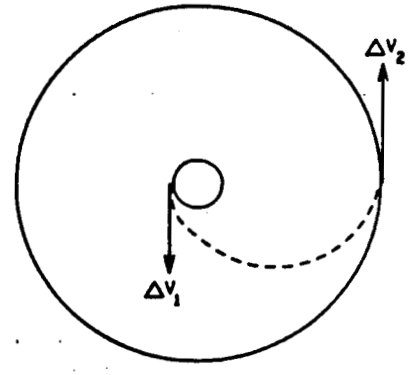

Figure 7.5

FINITE ELEMENT MODEL

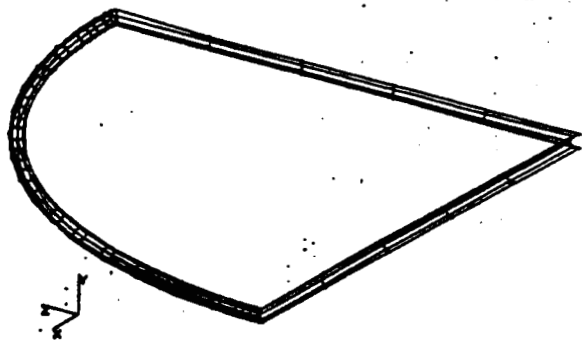

Figure 7.6

CASE 1: DISPLACEMENT

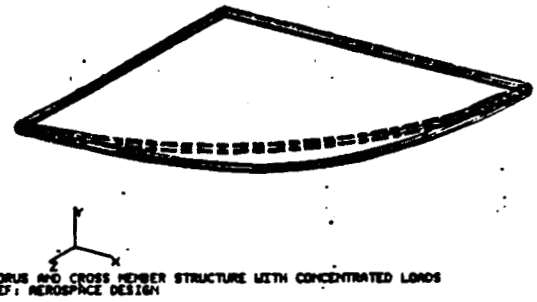

TORUS AND CROSS MEMBER STRUCTURE WITH CONCENTRATED LOADS
REF: AEROSPACE DESIGN

Figure 7.7

CASE 1: DISPLACEMENT

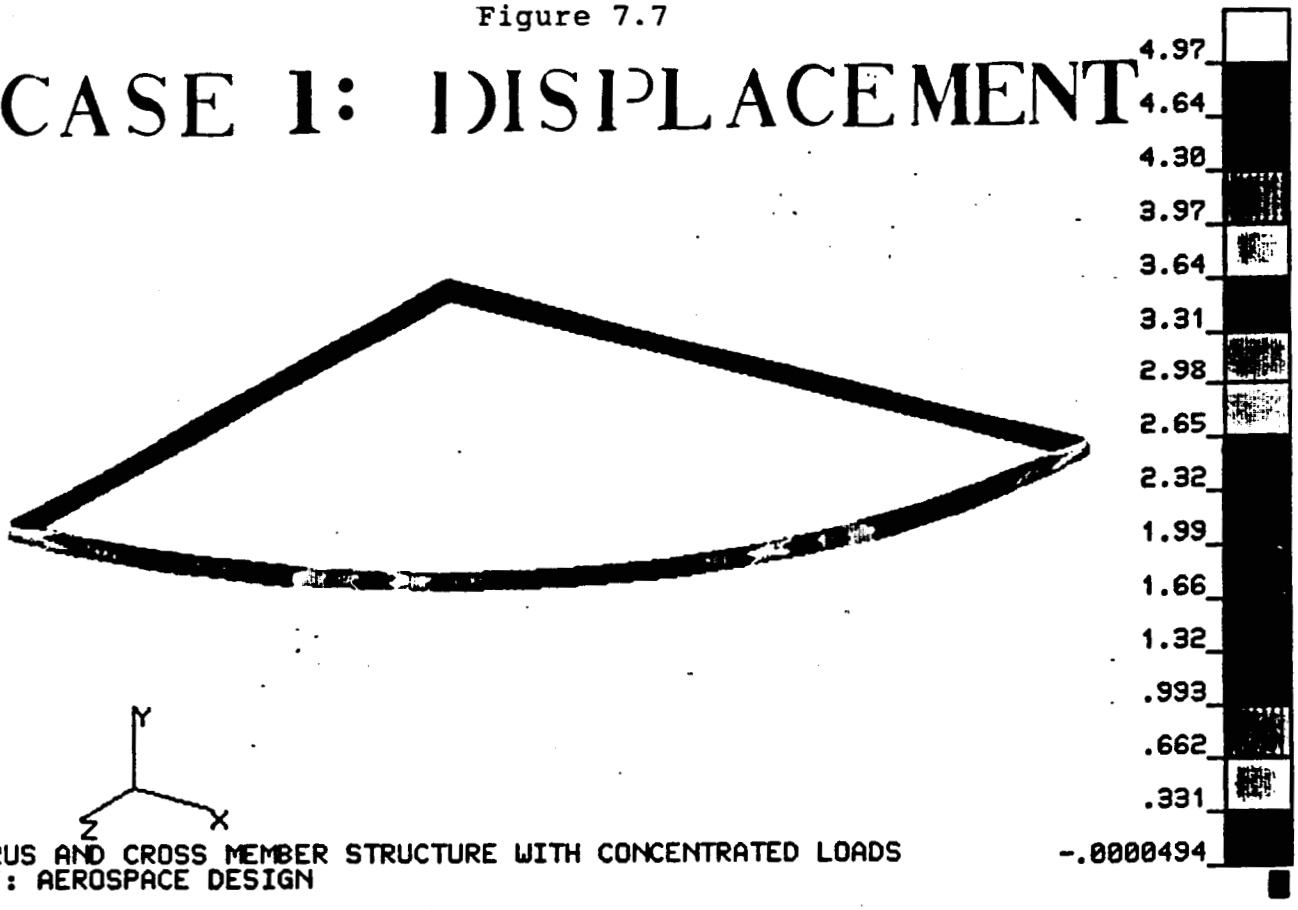

TORUS AND CROSS MEMBER STRUCTURE WITH CONCENTRATED LOADS
REF: AEROSPACE DESIGN

Figure 7.7

CASE 1: DISPLACEMENT

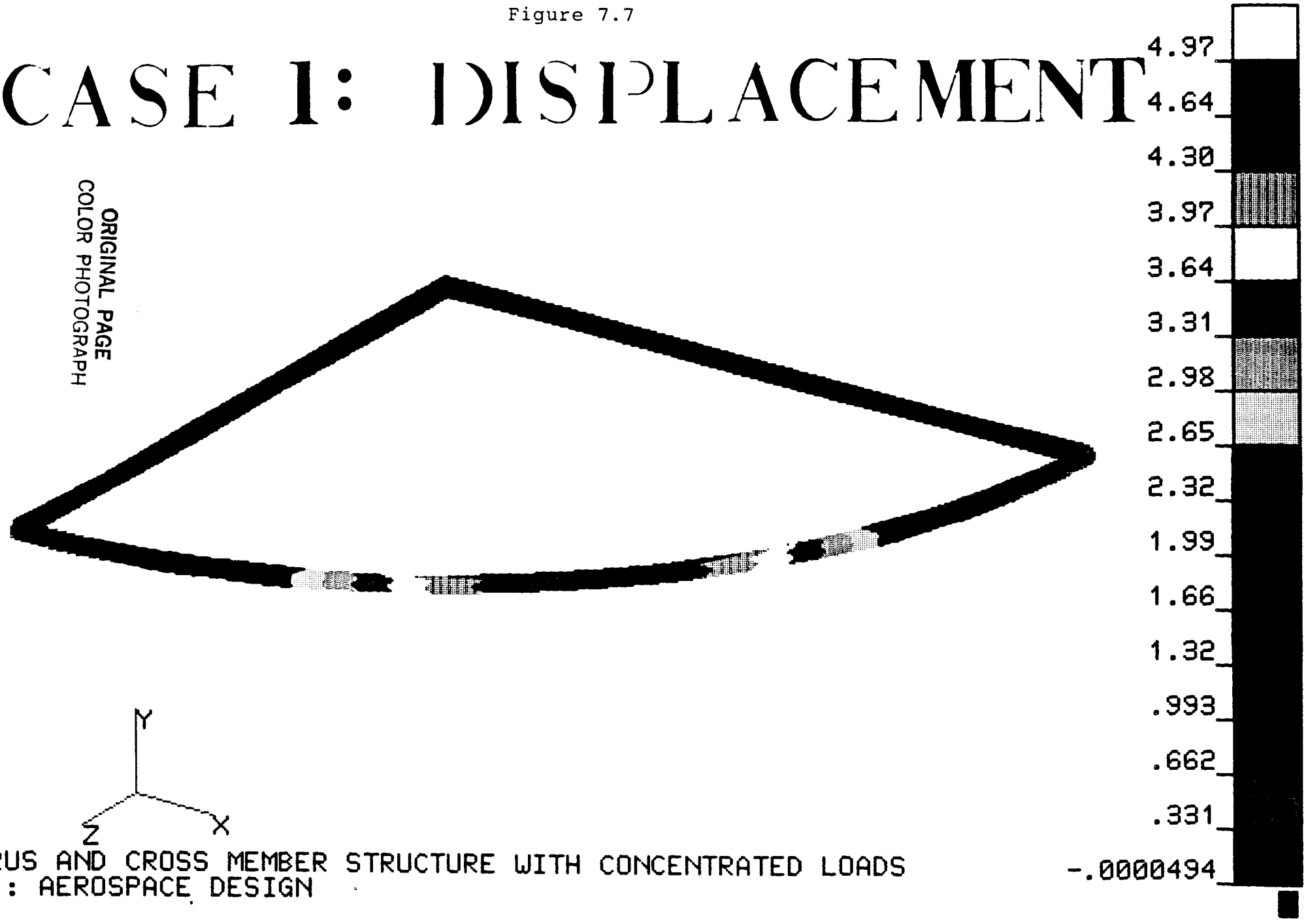

ORIGINAL PAGE
COLOR PHOTOGRAPH

TORUS AND CROSS MEMBER STRUCTURE WITH CONCENTRATED LOADS
REF: AEROSPACE DESIGN

Figure 7.8

NORMAL-X STRAINS

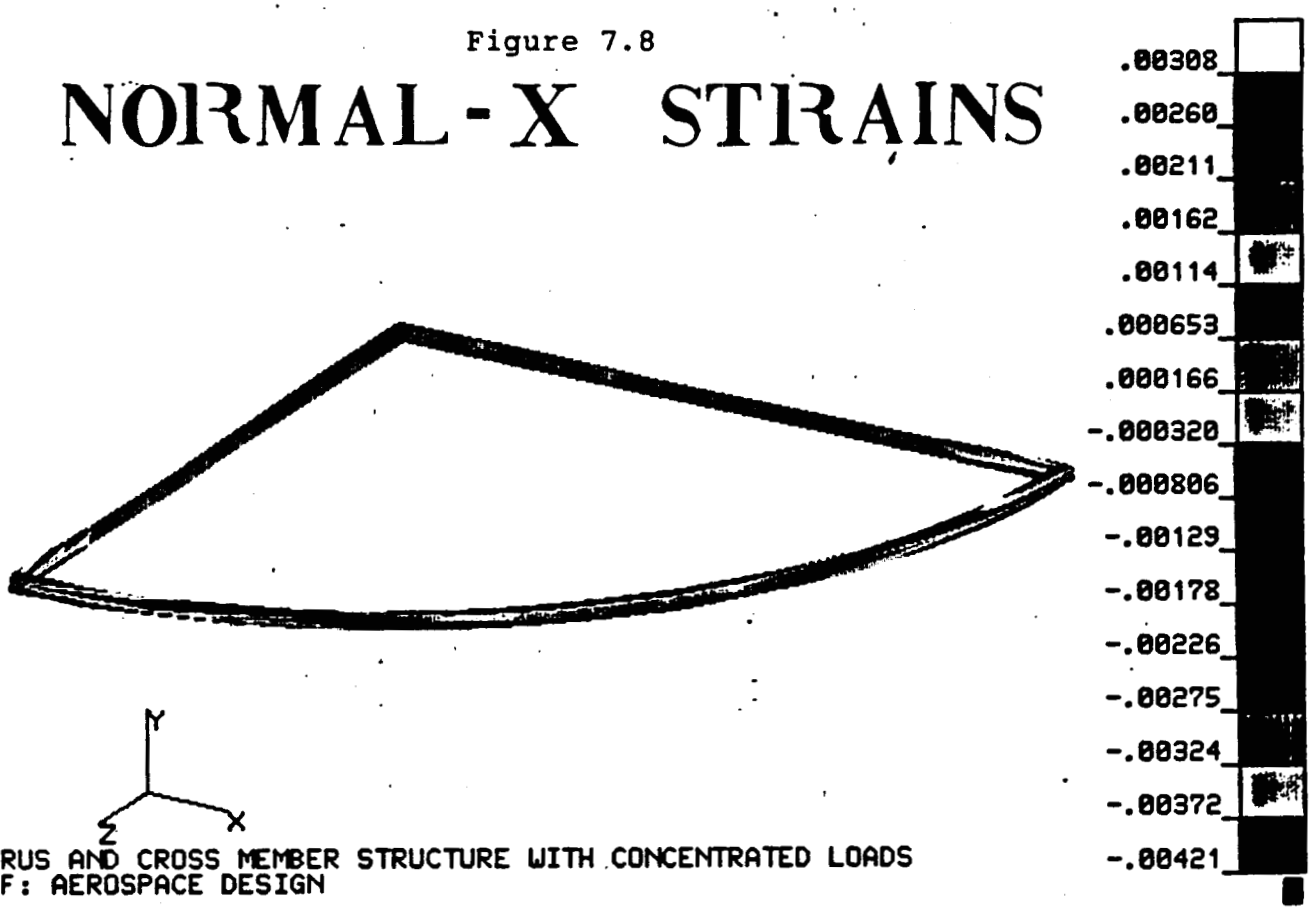

TORUS AND CROSS MEMBER STRUCTURE WITH CONCENTRATED LOADS
REF: AEROSPACE DESIGN

Figure 7.9

NORMAL-Y STRAINS

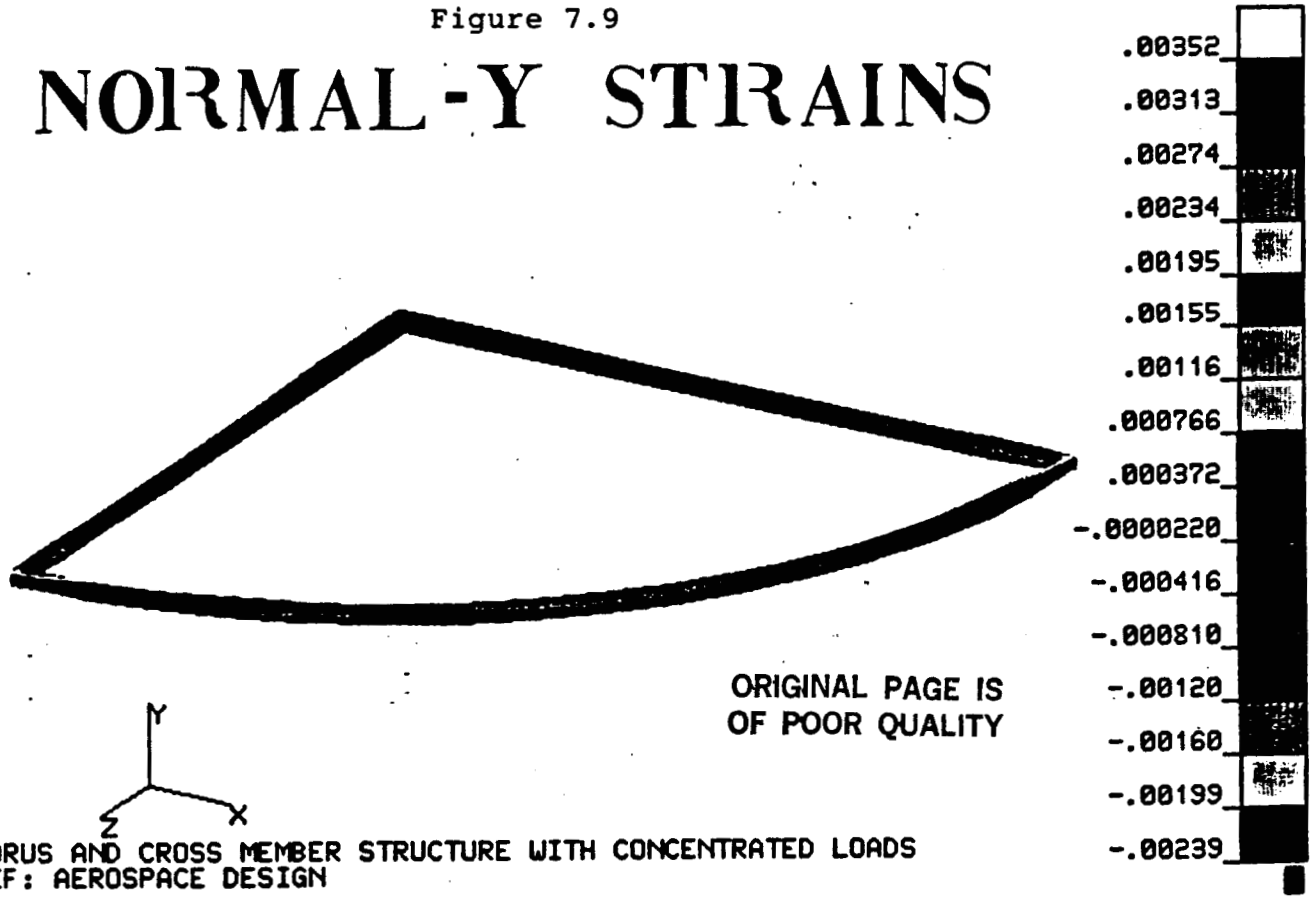

ORIGINAL PAGE IS
OF POOR QUALITY

TORUS AND CROSS MEMBER STRUCTURE WITH CONCENTRATED LOADS
REF: AEROSPACE DESIGN

ORIGINAL PAGE IS
OF POOR QUALITY

Figure 7.10

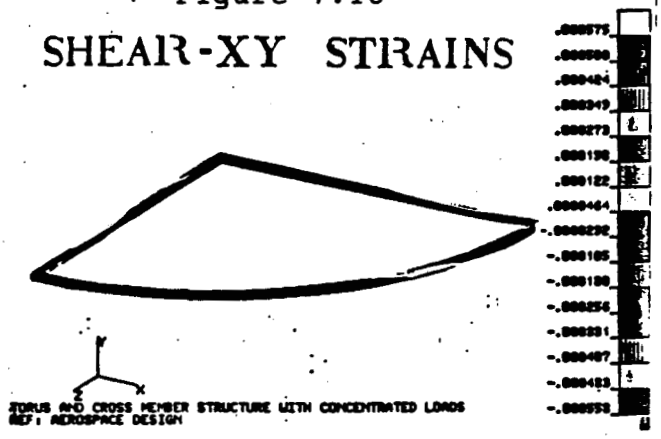

Figure 7.11

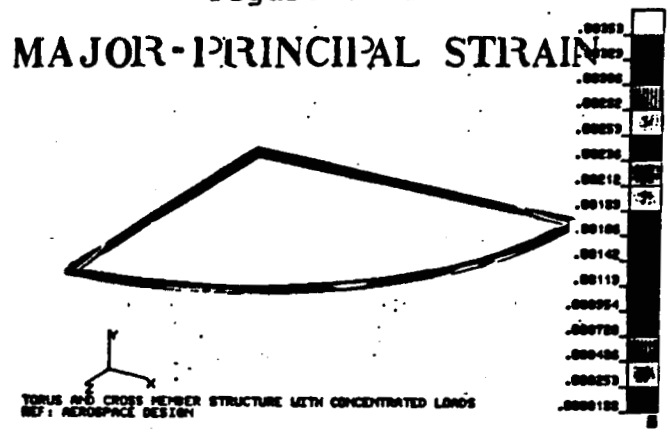

Figure 7.12

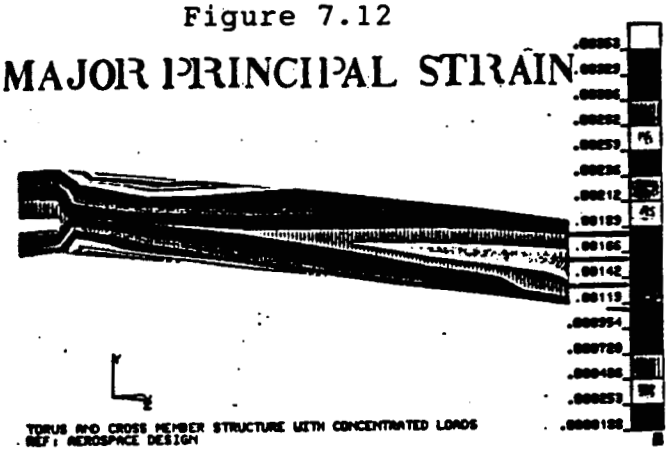

Figure 7.13

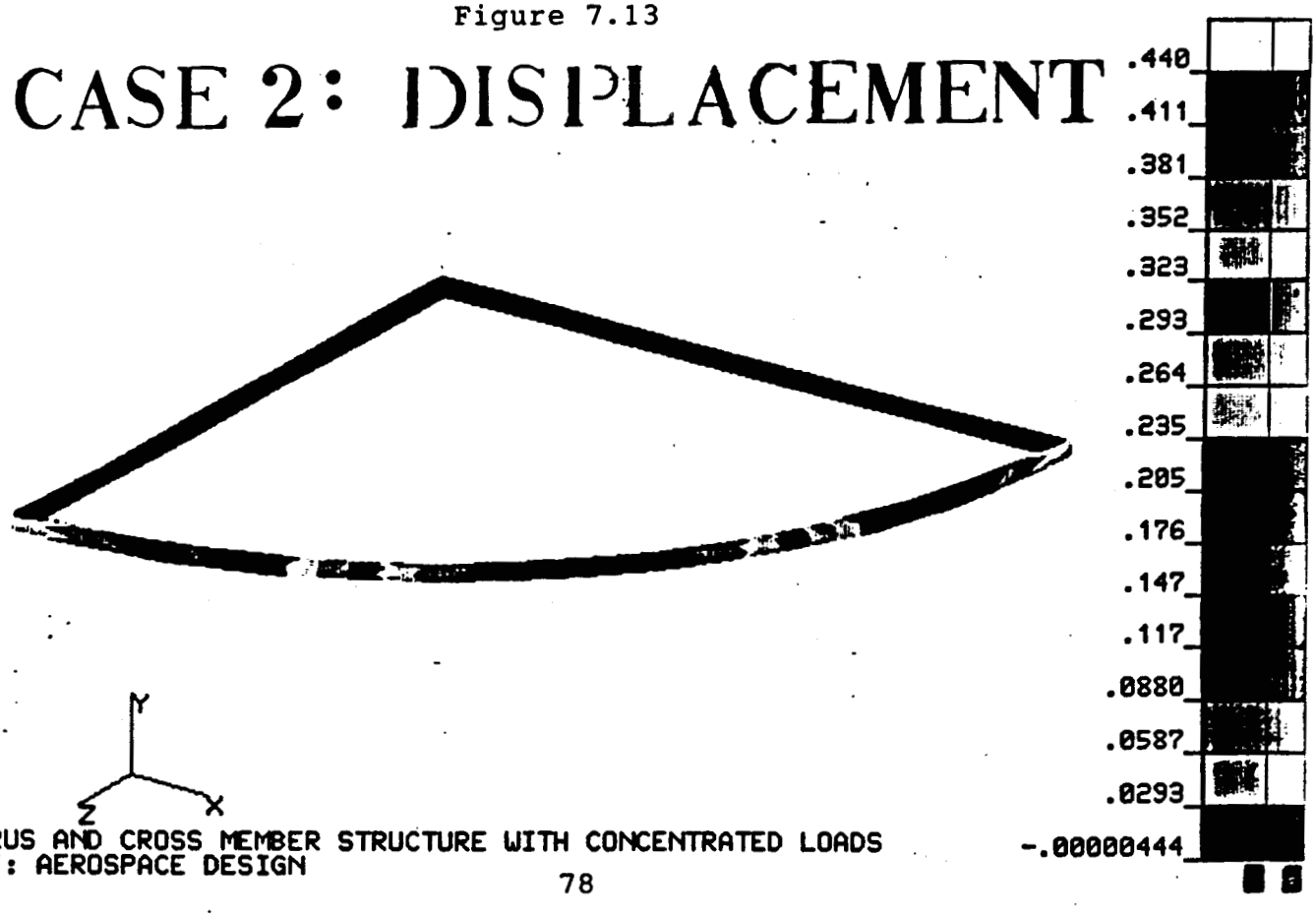

8.0 POWER SYSTEMS

There are different systems available that can provide ISAAC with the necessary power to be operational as a communications satellite. Furthermore, considerations for both the antennas and the control system need to be taken into account since they will have different power requirements.

8.1 Selection

Two systems were compared to supply ISAAC with power. They were solar arrays and nuclear fission. The different types of solar arrays looked at were honeycomb panels with stiffeners, flexible substrates with rigid frames, flexible fold-up blankets and flexible roll-up blankets. The difference between the solar arrays is the material from which the solar cells are placed on. The honeycomb panels with stiffeners have an end of life performance of 21.2 watts per kilogram (W/kg). These type of solar arrays are used on Intelsat V and Fltsatcom. The flexible substrates with rigid frames or ultra light panels have an end of life performance for a 7.12 kilowatt system of 39.3 W/kg. The flexible fold-up blankets have an end of life performance of 19 W/kg. The flexible roll-up blankets or flexible roll-up solar cell array (FRUSA) developed an end of life performance of 37.6 W/kg [Reference 1]. Nuclear fission was considered due to

its ability for producing large amounts of power, but it had a low performance of 6 W/kg [Reference 21]. Furthermore, this idea was dropped due to handling and possible political problems. In Figure 8.1 , the different power systems are compared. The best system is the ultra light panels because of there high performance coupled with compact ability. As improved solar cells are made the performance of all the solar arrays will increase.

8.2 Specifications

The power will be delivered by two wings of ultra light panels. Each solar panel will have an end of life power of 268 watts. The end of life is considered to be seven years for ultra light panels. Each panel is 1.15 by 3.3 meters (m) with an area of 3.795 square meters (m^2) . Each wing will have twenty panels and a yoke with a power output of 5360 watts (W) and with both wings of total 10,720 W. In Figure 8.2, the dimensions are shown for one wing both in extended and compact form. The length of one wing is 25.3 m with a width of 3.3 m. The compact form is .55 m thick with the length and height of 1.15 by 3.3 m. The total mass of the solar arrays is 272.4 kg and the total wing area is 167.0 m^2. The frame thickness on a wing is only .025 m. This has the volume for both the solar array wings being 4.368 cubic meters. Since the kapton substrate with the solar cells is only .0005 m thick, the panels in storage on the space shuttle will have vibration amplitudes of .0012 m [Reference 18].

8.3 Power Requirements

The power required by the antennas will be different than that required by the control systems. Still, the majority is required by the antennas, mainly for the transponders, and the rest is for such things as telemetry and attitude determination and control. Batteries are also investigated.

8.3.1 Antennas

The power required will primarily depend on how much wattage the receivers' amplifiers will need. Each antenna will have two transponders which have duel traveling wave tube amplifiers (TWTA). These TWTA are what boost the incoming signal from the receiver to the transmitter. Twenty-four of the antennas will have a capability of using the K_u band frequencies. Each K_u band TWTA will have an output power of 20 W and an input power requirement of 70 W. The K_u band range of frequencies is in a range of 12 to 14 gigahertzs (GHz). The other seventy-two antennas will be using C band frequencies. Each C band TWTA will have an output power of 10 W and required input power of 35 W. The C band of frequencies is in a range of 4 to 6 GHz.

The C and K_u band frequencies are what domestic and international telecommunications use. The use of C band requires less power because at lower wavelengths the signal is more clear, but it is becoming very crowded. The use of K_u band helps to expand satellite communications, but the higher wavelength costs more power to be clear [Reference

15]. The total needed for the TWTA will be 8400 W with 5040 W used for the C band TWTA and 3360 W used for the K_u band TWTA. Five percent of the total power will be saved for contingency which is 535 watts. The power required for ISAAC is shown in Figure 8.3. The specific weight of electronic power equipment, which goes with the power system, is 20 W/kg [Reference 21]. This has 536 kg of electronic power equipment added to the satellite.

Each antenna is assumed to have 1 W for transmitting power with a channel rate of 100 million bites per second [Reference 28]. The gain of the C band antennas are 57.5 decibels (dB) while the K_u band antennas are 64.9 dB. The effective isotropic radiated power (eirp) is the transmitting power times the gain. The eirp of the C band antenna are 57.5 decibel watts (dBW) with the K_u band being 64.9 dBW. The gain to temperature (G/T) ratio is assumed to be -5 decibel per kelvin (dB/K) [Reference 15].

8.3.2 Control Systems

The rest of the 1785 W will be for housekeeping. The housekeeping power goes to telemetry, command, ranging, attitude determination and control. The attitude determination and control involves both the pitch and the roll of ISAAC and it will be done with a combination of a momentum wheel and secondary thrusters. When ISAAC is boosted into geosychronous orbit, the momentum wheel will be rotated to equal the angular velocity of the Earth, which is

.0000727 radians per second (rad/s). When the correct angular velocity is reached, the secondary thrusters will be fired to dump the extra torque being generated by the wheel. The correct attitude determination will also require horizon sensors. Infrared detectors can sense the Earth from space because Earth radiates heat at 255 Kelvin (K) while space is only at 3 K [Reference 15]. All these systems would work through feedback and control loops allowing ISAAC to be kept at the correct position with an accuracy range of .1 degree. The mass of the attitude control subsystem is 335 kg [Reference 2].

Sun sensors will be used on the solar arrays in order to keep them collecting the maximum solar radiation. The solar array drive moves the arrays up to 15 degrees per hour. Telemetry on ISAAC is what is done to check on the status while command allows the ground control to add and execute received signals. The telemetry has both an omnidirectional antenna and bicone antenna. The omnidirectional antenna is used during the initial stages of ISAAC transfer to higher orbit then the bicone antenna is used for communication after the orbit has been stabilized. The commands are received on the omnidirectional antenna. The mass of the telemetry, command, and control subsystem is 180 kg [Reference 1]. The frequency range of the telemetry signal is 137 to 138 megahertz (MHz) with a command frequency range of 1525 to 1540 MHz. Both telemetry and command signals will be encoded to eliminate unauthorized signals.

8.3.3 Batteries

A satellite in geosynchronous orbit will pass through the dark side of the Earth for up to 72 minutes each year. Presently, nickel cadmium batteries are being used and they have a performance of 15 W/kg. However, a new battery just starting to be used is the nickel hydrogen battery. The nickel hydrogen type have a performance of 30 watt-hours per kilogram and only degrade approximately 30 percent over ten years [Reference 2]. From this performance value the mass of the batteries would be 428.8 kg for 10,720 W.

The brain will be the main control unit and will be located at the center of ISAAC. Thus, the batteries, electronic equipment, telemetry and attitude control will be placed there. The omnidirectional and bicone antennas will be placed facing Earth.

The total and breakdown weight for ISAAC can be seen in Figure 8.4. Thus, the combined mass for the control unit is 1500 kg, and the thermal control for the unit is 30 kg. The thermal control involves heating pipes which keep the equipment at the correct temperature. The batteries need to be between 273 and 298 K with the rest of the equipment being between 273 and 328 K [Reference 1].

ORIGINAL PAGE IS
OF POOR QUALITY

Figure 8.1

POWER SYSTEMS

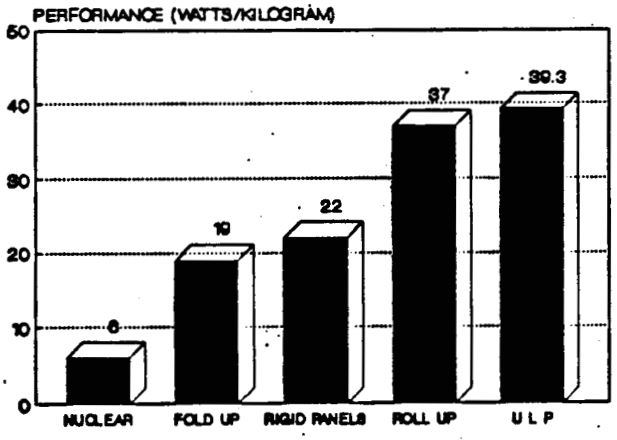

Figure 8.2

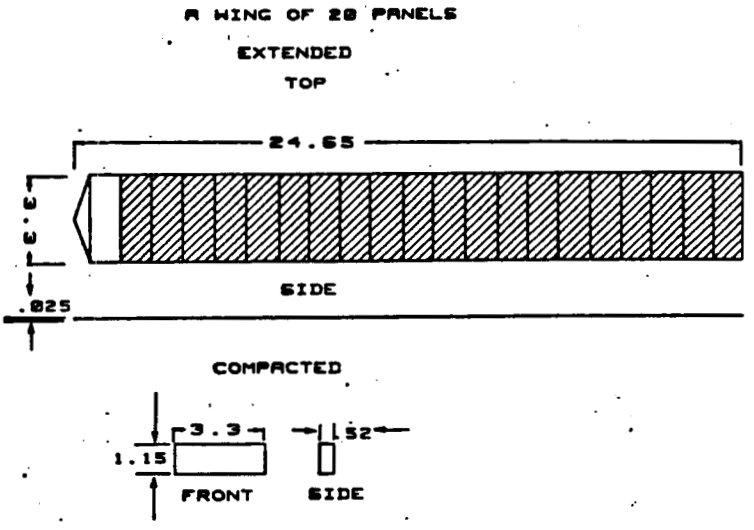

Figure 8.3

POWER REQUIRED
(WATTS)

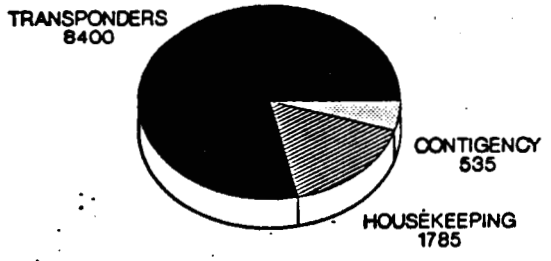

TOTAL 10720

Figure 8.4

ISAAC'S WEIGHT
(KILOGRAMS)

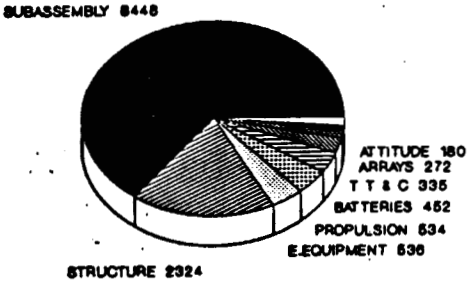

TOTAL 13081

9.0 VARIOUS APPLICATIONS

As stated previously, ISAAC has been initially designed as a satellite for two-way communications with many low-power stations on the ground. However, other mission requirements could be met with only minor modifications. These missions include a communications satellite for distributing wide band television directly to very small home receivers, an extension of an earth-based very long baseline interferometer to achieve higher resolution radio images of stars than is possible with Earth-based arrays, a high resolution microwave radiometer for studying weather phenomena, or a microwave power transmitting antenna portion of a power satellite.

9.1 Wide-band Television Distributor

To change ISAAC, which is a two-way communications antenna array, to a satellite which distributes television, but keeps the present structure, would require a few modifications. The first would be to set up one group of antennas to receive the master signal, while the rest of the antennas would transmit. The transmitting antennas would have to be connected by thermally insulated coaxial cables to transfer the signals. A main control unit would have to be used to sort through the different frequencies and then channel them to the correct antennas. The frequencies of the transmitting antennas need to be like those used for

television, which is the C band range [Reference 15].

The power requirement for the wide range television array would differ from ISAACs. The same number of transponders, which is 192, will have a power requirement of only 6720 watts. This has the solar arrays', electrical equipment's, and batteries' weight reduced. A total power of 9112 watts is needed, which will have 34 panels being used in two wings. The area for both wings is 136.6 square meters with a weight of 231.8 kg. The mass of the batteries is 364 kg and the electrical equipment is 455.6 kg. Both the telemetry and attitude control stay the same.

One of the major disadvantages is that most of the revenue comes from telephone, data and records transfer. In Figure 9.1, the revenues for Intelsat in 1982 are shown, with 82 percent coming from telephones and data while only 6 percent is from television [Reference 2].

9.2 Radio Interferometer

To change ISAAC to an extension of an earth-based very long base interferometer would also require modifications. First, the satellite would have to be turned to face space, except that one group of antennas would face the earth. When using an interferometer, to be effective the antennas must far apart because the farther the distance between antennas the better the resolution. This is because resolution is defined as wavelength over the maximum distance between

antennas, and thus the maximum distances needed would be in the thousands of kilometers [Reference 21]. If an antenna array on earth and an antenna array satellite could work together, or if a group of satellites work together, this would give the distances needed to be effective.

Still, the satellites' arrays need to have powerful electrical equipment, and computers are needed to link the different sources together. The data will have to be accurately recorded with hydrogen clocks to keep precise time, and a large power source is needed because the incoming signal will need to be boosted twice, both times up to ten to one thousand times. The satellite will also have to have an accurate pointing system in order to locate the source, which involves a star tracker. (A star tracker uses two or more fixed stars to measure positions from.) Furthermore, more fuel will be needed so that the satellite will have the ability to maneuver to different positions [Reference 13].

9.3 Weather Satellite

Another potential use of our large antenna array satellite is to use it as a high-resolution microwave radiometer for studying weather phenomena. Since the spacecraft will be operating at GEO, this means that the satellite will watch the weather change around a certain area continuously (i.e. the United States).

To change the configuration to a weather satellite requires three additional instruments. They are the

microwave radiometer, sounding sensor, and a data relay system. The radiometer measures the Earth's infrared and reflected solar radiance. It will be operating at various microwave lengths to measure temperature, ozone, water vapor.... etc. This is done by placing a multi-frequency feed horn off the main axis of the off-set parabolic dish. The purpose of the sounding sensor is to obtain profiles of temperatures and various gases as a function of height. Furthermore, the data relay system records data collected and transfers it back to Earth. All these instruments will be installed at the central control unit of each set of parabolic dishes, except for the data relay system which will be placed at the central control module of the whole structure (located at the center of the structure). The data recorded from each individual box will be transferred here, and then it will be beamed down to a ground station. The radiometer will be operating at the solar-band in the microwave region [Reference 26].

9.4 Power Satellite

Another application of our large antenna array satellite is to transform it to a power satellite for energy usage. The satellite, with its surface constantly facing the sun, would be covered with a " blanket " of solar cells. The solar cells would receive radiation from the sun and convert it to an electrical current by means of photovoltaic effect.

The current would then be transformed into electromagnetic waves at a frequency of 2450 MHz in the microwave region of the spectrum. The microwaves would then be beamed down to Earth [Reference 8].

As far as the technical aspect is concerned, the solar cells will be made of silicon. This is because silicon cell arrays have been used successfully in GEO on communications and other satellites during the last two decades. Klystron tubes would be the source for transmitting power from space to Earth. It can operate in both pulsed and continuous-wave modes over a wide range of frequencies, and, in many cases, it would produce higher power output than required. This will be placed in the central control unit of each set of parabolic dishes. Also, a transmitting antenna would be needed to beam the microwaves down to earth. This will also be placed also at the central control units. All the microwaves will be beamed down to Earth at a common location. Down on Earth, the ground facilities would convert the microwaves received to proper current and use it to generate useful power [Reference 8].

C-2

Figure 9.1

INTELSAT REVENUES

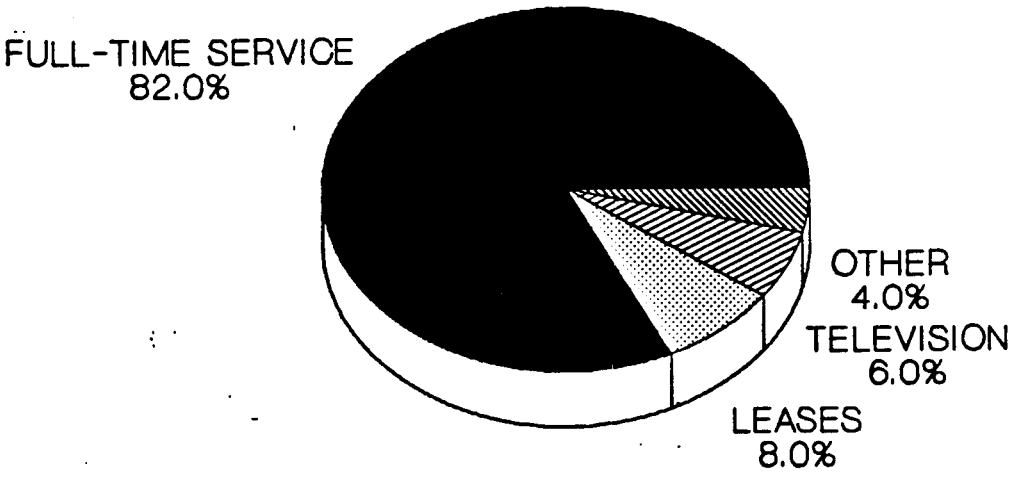

FROM REFERENCE 2

10.0 ADMINISTRATIONS

The managerial organization for such a large project needs to be considered, for that is often the key to success or failure of the project. The success also depends on the ability to keep the production on time and on cost. Thus, there is an importance placed on the production schedule and cost estimates, yet without negligence or at the expense of quality.

10.1 Management Organization

The project's management organization is depicted in Figure 10.1. It was decided to go with a matrix organization, thus providing for a wonderful built-in checks and balances system. Although all organizations have their problems, a matrix-type organization has proven itself to be very efficient in industry [Reference 23]. Project managers will be in charge of the different subsystems of the satellite, while line managers will be in charge of the different departments. This way, there will be constant interaction between everyone involved.

Furthermore, as each phase of the production is completed, the groups can begin to work on a new portion of the production, thus saving cost in payroll (less employees will needed to be hired). Of course, it is assumed that if it is cheaper to obtain an existing product (i.e. the

materials, or maybe even the reflectors from Contraves), then that would be the appropriate line of action.

Quality assurance will be an essential part of the program, with continual quality assurance review meetings, along with regular design review meetings. There will also be strict adherence to all specifications and standards.

10.2 Production Schedule

A schedule for the production of ISAAC has been developed and can be seen in Figure 10.2. It was decided to use a Gantt (Milestone) Chart so that all key completion points throughout the production could be easily verified. It is a very good method for keeping production on time or for finding out, at an early enough date, that production is falling behind schedule [Reference dd].

10.3 Cost Analysis

The cost of ISAAC is difficult to estimate, but using today's satellites' costs can allow for a rough estimate on the cost and the cost performance. Today's satellites cost approximately 75,000 dollars per kilogram [Reference 15]. The electronic controls, which are located at the control box, weigh about 1500 kg. This makes the cost for the electronic controls to be 111 million dollars. The solar arrays weigh 272 kg which make them 21 million dollars.

Each antenna subassembly is 352 kg with the antennas

weighing 248 kg, and the rest of the electronics and structure are 102 kg. In Figure 8.4, the weight breakdown of ISAAC is shown. Using today's cost, the cost for an antenna subassembly is 7.6 million dollars, and thus the total cost for each antenna subassembly is approximated to be 8 million dollars. Since there are 24 individual subassemblies, the total cost for the whole antenna subassembly is 192 million dollars.

Each antenna has 226 m^2 of surface material. The price of the kevlar is known which is 22 dollar per square meter, but the manufacturing costs are unknown. Still, the kevlar in the antenna is 5200 dollars, and the total cost is inflated to 100,000 dollars to include the other costs [Reference 11].

The inflatable structure covers an area of 4,840 square meters, which is also made from kevlar. Thus, the kevlar cost for the torus is 114,000 dollars, but this does not include the outer covering or manufacturing costs. Therefore, the structure cost is inflated to be 10 million dollars.

These totals, plus five percent added, give ISAAC a rough cost of 350 million dollars. Even though the cost seems high , the cost performance is low. The cost performance is the total cost per number of transponder per life span. Intelsat has made a cost performance line for their satellites plus future ones. In Figure 10.3, the cost performances of different satellites are shown. Intelsat IV

cost 13.4 million dollars and had a cost performance of 1 million dollars per transponder per year, while Intelsat VI cost 140 million dollars with a cost performance of 125,000 dollars per transponder per year [Reference 2]. The estimate performance of ISAAC with 192 TWTA and a 10 year life span is 93,000 dollars per transponder per year, which is what the Intelsat corporation expects there future platforms to be.

The cost estimate does not include launching or building in space. In the future, it will cost about 12,700 dollars per kilogram to have a satellite launched on the space shuttle which costs the 15,348 kg ISAAC 195 million dollars [Reference 12]. For an astronaut to work in space costs about 15,000 dollars per hour, so for one week of 12 hours each with two astronauts would cost at least 2.5 million dollars [Reference 28]. Insurance is priced to 8 percent of the value of the in orbit satellite. For ISAAC, this would cost 43 million dollars. Thus, the total initial deployment cost would run 580 million dollars, depicted in Figure 10.3.

ORIGINAL PAGE IS
OF POOR QUALITY

Figure 10.1

Matrix Organizational Chart
For The Isaac RIS Structure
Antenna System

Project	Director of R&D	Director of Eng.	Director of Manu.	Director of Testing	Director of Quality Control
Toroid	Research and Developement Department	Engineering Department	Manufacturing Department	Testing Department	Quality Control Department
Reflector Subassemblies					
Power Systems					
Propulsions					
System Integration					

Figure 10.2

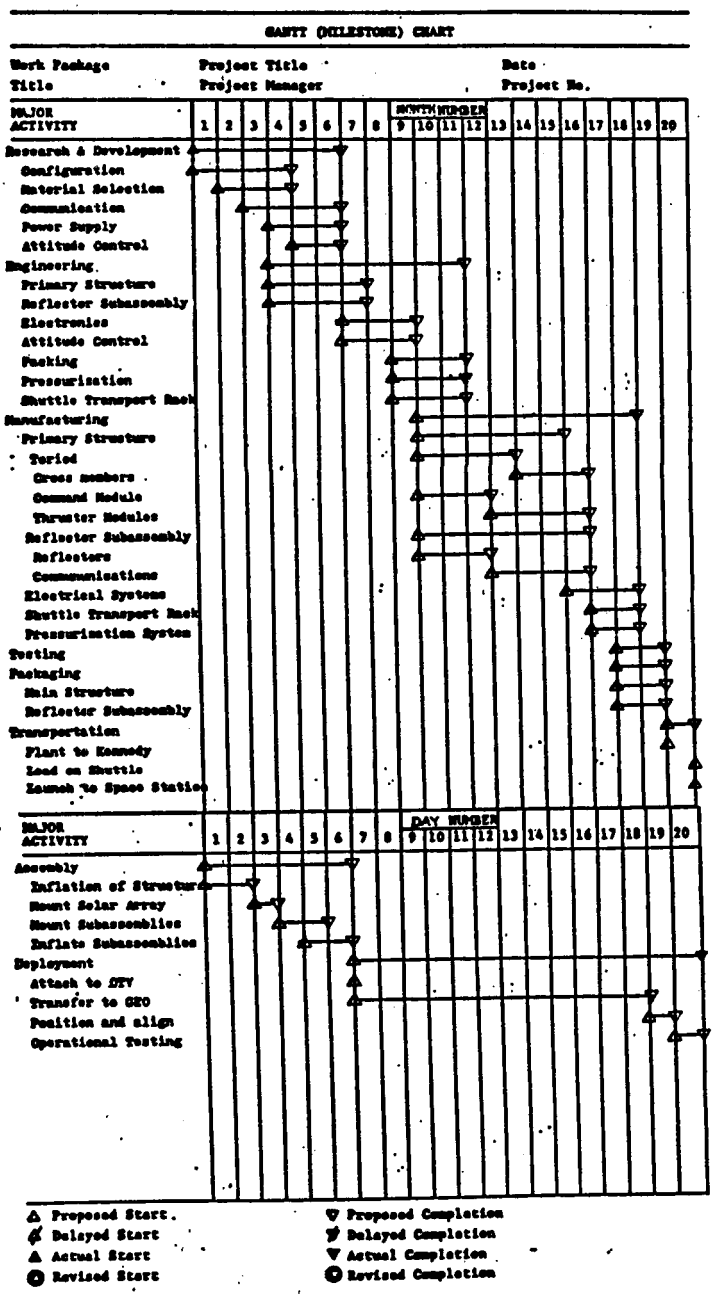

Figure 10.3

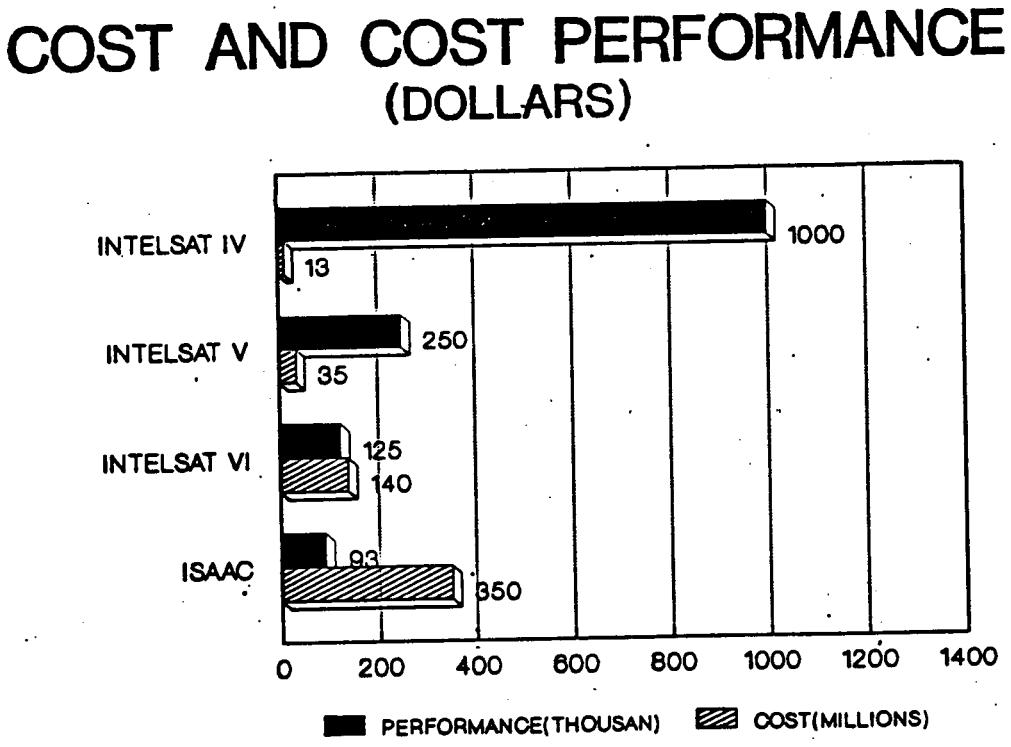

Figure 10.4

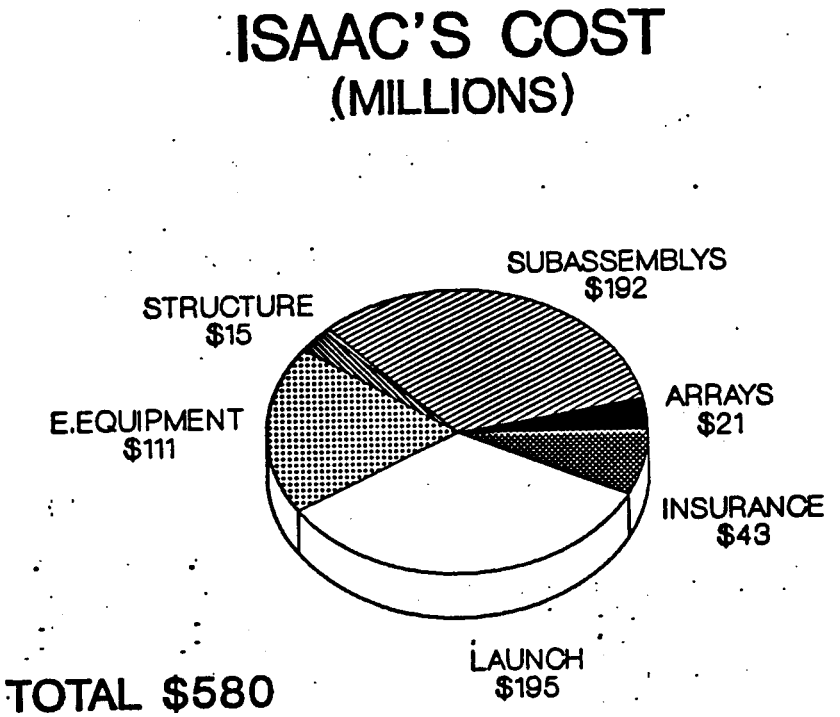

11.0 CONCLUSIONS

This design of an antenna array satellite using rigid inflatable structure technology provides for a satellite for two-way communications with many low-power stations on the ground. The design, ISAAC, consists of a phased array of many antennas with an equivalent aperture greater than 100 m in diameter, as per request of the RFP. The array will be constructed using rigid inflatable structure technology, as will the structure that will carry the array, thus taking the most advantage of the technology.

The initial design meets all design requirements and constraints set forth as part of the competition:

1) The main structure and the reflector subassemblies are easily packaged into minimum volumes to be stored in the Space Shuttle cargo bay for transportation to the Space Station. In fact, the structures and everything required for normal operations can be brought to the Space Station in one trip.

2) The structure and antennas are easily inflatable in a zero- or micro- g environment and use an environmentally safe, nontoxic gas.

3) The structures will be well cured before the inflation gas leaks out. Furthermore, the structural properties will not change significantly with time.

4) NASTRAN analysis proves the structure will be able to withstand typical propulsion stresses during boost to GEO and in normal operations.

5) Uneven thermal heating and mechanical loading will not hinder any operations.

6) Micrometeorite impacts will not cause significant structural damage.

7) The surface coatings are incorporated into the initial manufacturing and thus require no in-orbit application.

Furthermore, other missions can easily be met with only minor modifications to the initial design.

The initial step in the design process was to fully understand the requirements presented in the 1988 AIAA/Allied Corporation Team Design Competition. Thus, the mission profile could be defined and the critical design requirements could be identified. Trade off studies were performed to decide on the final configuration and all other subsystems involved. Performing a structural analysis was the final step of verification of the validity of the design. Thus, the design team feels that ISAAC optimally satisfies all the design constraints and requirements.

REFERENCES

[1] Agrawai, Brij N., Design of Geosynchronous Spacecraft, Prentice-Hall Inc., Englewood Cliffs, NJ, 1986.

[2] Alper, Joel and Delton, Joseph N., ed., "The INTELSAT Global Satellite System", American Institute of Aeronautics and Astronautics, New York, 1984.

[3] American Cyanamid technical information, "Advanced Composites and Prepegs", American Cyanamid Co., 1988.

[4] Bernasconi, M. C., "Development of a 2.8 m offset antenna reflector using inflatable, space-rigidiized structures technology", ESA Proceedings of the Second ESA Workshop on Mechanical Technology for Antennas, p 31-37, Aug. 1986.

[5] Bernasconi, M. C., "Large spaceborne antenna reflectors using inflatable space rigidized structures", ESA Workshop on Mechanical Technology for Antennas, p 31-36, Sept. 1984.

[6] Burlington Glass Co. technical information, "Kevlar Cloth Properties", Burlington Glass Co., 1988.

[7] Chapman, Alan J., Heat Transfer, Macmillan Publishing Co., 1984.

[8] Committee on Satellite Power System, Electric Power from Orbit: A Critique of a Satellite Power System, National Academy Press, Washington D.C., 1981.

[9] Contraves, "Study on Large, Ultra-light Long-life Structures in Space", Contraves, 1982.

[10] Dunnet, L.T., "An Introduction to Space", her majesty stationary office, London, 1968.

[11] Dupont technical information, "Characteristics and Uses of Kevlar 29 Aramid", Dupont, 1976.

[12] Easterbrook, Gregg, "Big Dumb Rockets", Newsweek, CX, August 17, 1987.

[13] Fanti, R. and others, ed., VLBI and Compact Radio Sources, D. Reidal Publishing Co., Holland, 1984.

[14] Freeman, Roger L., Telecommunications Transmission Handbook, Second Ed., John Wiley & Sons, New York, 1981

[15] Fthenakis, Emanuel, Manual of Satellite Communications, McGraw Hill Book Co., New York, 1984.

[16] Hesse, Walter H., McDonald, Robert L., Space Science, Charles E. Merrill Publishing Co., Ohio, 1970.

[17] Higdon, A., Mechanics of Materials, John Wiley & Sons, New York, 1985.

[18] Jarett, David, ed., "Satellite Communication: Advanced Technologies", American Institute of Aeronautics and Astronautics, New York, 1976.

[19] Jones, R.M., Mechanics of Composite Materials, Hemisphere Publishing, New York, 1975.

[20] Kaplan, Marshall, Modern Space Dynamics and Controls, John Wiley & Sons, New York, 1976.

[21] McGraw-Hill Encyclopedia of Science and Technology, McGraw-Hill, New York, 1987.

[22] Reibaldi, G. G. et al, "Inflatable space rigidized reflector development for land mobile missions", 11th Communication Satellite Systems Conference Technical Papers, p 533-538, March 1986.

[23] Shannon, Robert E., Engineering Management, John Wiley & Sons, New York, 1980.

[24] Sierracin/Intrex Film technical information, "Properties of Polymide Films", Sierracin/Intrex Film, 1988.

[25] Sutton, George P., Rocket Propulsion Elements, 5th ed., John Wiley & Sons, 1986.

[26] Taggart, Dr. Ralph E., New Weather Satellite Handbook, Wayne Green Inc., 1981.

[27] Turnill, Reginald, ed., Jane's Spaceflight Directory, Jane's Publishing Inc., New York, 1987.

[28] Woodcock, G. R., Space Stations and Platforms, Orbit Book Co., Florida, 1986.

[29] Yang, T. Y., Finite Element Structural Analysis, Prentice-Hall, New Jersey, 1986.

APPENDIX A

Sample NASTRAN Output

N A S T R A N E X E C U T I V E C O N T R O L D E C K E C H O

```
 MSC, TORUS $ TEW 05-MAY-88
IL 24
ME 400

   ******************************************************
   ** ALTER STATEMENTS FOR POSTPROCESSING WITH PATRAN **
   ******************************************************

      STATICS

AD 9 $ RF24D81 RF24D79
BEGINNING OF RF ALTER 24$81
+ + + + + + + + + + + + + + +          12 JULY 1982        + + + + + +        + +

      STRESSES AT GRID POINTS FOR PRINTOUT

TER 176 $
RAML   POSTCDB//C,N,PRES////V,N,NOPOST $
ND     ENDPOST,NOPOST $
RAML   OES1//C,N,PRES////V,N,NOPOST $
ND     ENDPOST,NOPOST $
TSET   POSTCDB,EQEXIN,ECT/PLTP,PLTPARP,CPSETP,ELSETGP/V,N,NSIL $
STR1   POSTCDB,BGPDT,ECT,CSTM,ELSETGP,EPT/EGPSF/S,N,NOEGPSF $
RAML   EGPSF//C,N,PRES////V,N,NOPOST $
ND     ENDPOST,NOPOST $
STR2   CASECC,EGPSF,GPL,OES1/OGS1,///C,N,STATICS $
P      OGS1//S,N,CARDNO $
BEL    ENDPOST $
END OF RF ALTER 24$81
 BEGINNING OF ALTER - RF24D79  - FOR STRESS RECOVERY ON INDIVIDUAL
   PLIES FOR LAYERED COMPOSITE ELEMENTS.
 STRESSES AND FAILURE INDICES FOR ALL THE PLIES IN AN ELEMENT
   CAN BE OBTAINED. STRESSES FOR NON-COMPOSITE ELEMENTS WILL BE
   OUTPUT IN OES1 FILE; STRESSES FOR COMPOSITE ELEMENTS WILL BE
   OUTPUT IN OES1C FILE; FAILURE INDEX TABLE FOR COMPOSITE ELEMENTS
   WILL BE OUTPUT IN OEFIT TABLE.
 SORT OPTION IS AVAILABLE TO SORT STRESSES FOR COMPOSITE ELEMENTS
   - USE NUMOUT1 AND BIGER1 PARAMETERS.
 SORT OPTION IS AVAILABLE TO SORT FAILURE INDICES FOR COMPOSITE
   ELEMENTS - USE NUMOUT2 AND BIGER2 PARAMETERS.
 ELSTRESS AND ELFORCE CASE CONTROL KEYWORDS TO REQUEST STRESSES
   AND FORCES FOR THOSE ELEMENTS (WHOSE PLY STRESSES AND FAILURE
   INDICES ARE DESIRED) MUST BE PRESENT IN THE CASE CONTROL DECK.
TER    203
ND     LBLCOMP,NOCOMP $
R2     CASECC,CSTM,MPT,DIT,EQEXIN,SIL,ETT,EDT,BGPDT,PGG,QG,UGV,ESI,
       XYCDB/ , , ,OES1A,OEFDUM, /  STATICS  / S,N, NOS/2 $
RCOMP  CASECC,MPT,EPT,ETT,ESI,OES1A,OEF1,DIT/ES1C,EFIT/ $
RSORT  ES1C,/OES1C/C,Y,NUMOUT1=-2/C,Y,BIGER1=0.0 $
```

N A S T R A N E X E C U T I V E C O N T R O L D E C K E C H O

```
STRSORT  EFIT,/OEFIT/C,Y,NUMOUT2=-2/C,Y,BIGER2=0.0 $
OFP      OES1C,OEFIT,,,//S,N,CARDNO $
LABEL    LBLCOMP $
$  END OF ALTER RF24D79
ALTER 176 $
VECPLOT      UGV,BGPDT,EQEXIN,CSTM,CASECC,/UGVBASIC//0/1 $
SDR2         CASECC,CSTM,MPT,DIT,EQEXIN,,ETT,EDT,BGPDT,PGG,QG,
             UGVBASIC,EST,/,,OUGV1PAT,,,/STATICS/S,N,NOSORT2/
             V,N,NOCOMP $
OUTPUT2      OUGV1PAT,OES1//-1/11/V,N,Z $
$
$       ELEMENT STRAIN RECOVERY
$
ALTER 215    $
VECPLOT      UGV,BGPDT,EQEXIN,CSTM,CASECC,/UGVBASIC//0/1 $
SDR2         CASECC,CSTM,MPT,DIT,EQEXIN,,ETT,EDT,BGPDT,PGG,QG,
             UGVBASIC,EST,/,,OUGV1PAT,,,/STATICS/S,N,NOSORT2/
             V,N,NOCOMP $
OUTPUT2      OUGV1PAT,OSTR2//-1/11/V,N,Z $
$
$       GRID POINT FORCES
$
ALTER 189    $
VECPLOT      UGV,BGPDT,EQEXIN,CSTM,CASECC,/UGVBASIC//0/1 $
SDR2         CASECC,CSTM,MPT,DIT,EQEXIN,,ETT,EDT,BGPDT,PGG,QG,
             UGVBASIC,EST,/,,OUGV1PAT,,,/STATICS/S,N,NOSORT2/
             V,N,NOCOMP $
OUTPUT2      OUGV1PAT,OGPFB1//-1/11/V,N,Z $
CEND
```

C A S E C O N T R O L D E C K E C H O

```
CARD
COUNT
 1      TITLE=TORUS AND CROSS MEMBER STRUCTURE WITH CONCENTRATED LOADS
 2      SUBTITLE=REF: AEROSPACE DESIGN
 3      $ INFLATABLE SPACE ANTANNE STRUCTURE
 4      ECHO=NOSORT
 5      LOAD=40
 6      DISPLACEMENT=ALL
 7      SPCFORCE=ALL
 8      FORCE=ALL
 9      GPFORCE=ALL
10      STRAIN=ALL
11      STRESS=ALL
12      GPSTRESS=ALL
13      OUTPUT(POST)
14      SET 1=ALL
15      SURFACE 11 SET 1 NORMAL Z
16      BEGIN BULK

          INPUT BULK DATA CARD COUNT =     479

       TOTAL COUNT=   434
```

EXAMPLE OF RESULTS FOR ELEMENT 13

VECTOR RESULTANT

	T1	T2	T3	R1	R2	R3
1	-4.7235851E+00	-3.3648309E+02	-3.5573047E-01	1.6682791E+04	-8.7052994E+01	-1.6846219E+04

D I S P L A C E M E N T V E C T O R

POINT ID.	TYPE	T1	T2	T3	R1	R2	R3
130	G	1.741507E-01	-6.144345E-01	-2.700033E-03	0.0	0.0	0.0
131	G	-1.174624E-02	-1.752778E-01	-9.182173E-03	0.0	0.0	0.0
148	G	1.741359E-01	-6.074618E-01	0.0	0.0	0.0	-3.426432E-01
150	G	4.831297E-03	-2.084866E-01	0.0	0.0	0.0	5.613866E-02

F O R C E S O F S I N G L E - P O I N T C O N S T R A I N T

POINT ID.	TYPE	T1	T2	T3	R1	R2	R3
130	G	0.0	0.0	0.0	-6.026096E+00	-3.447977E+00	9.246879E+00
131	G	0.0	0.0	0.0	-4.270725E+00	6.266553E+00	2.769398E+01
148	G	0.0	0.0	8.845583E+03	-8.976212E-01	4.652664E-01	0.0
150	G	0.0	0.0	3.243218E+04	7.406997E+01	2.702240E+00	0.0

F O R C E S I N Q U A D R I L A T E R A L E L E M E N T S (Q U A D 4)

LEMENT	- MEMBRANE FORCES -			- BENDING MOMENTS -			- TRANSVERSE SHEAR FORCES -	
ID	FX	FY	FXY	MX	MY	MXY	QX	QY
13	-2.184967E+04	5.075522E+02	-1.699792E+03	-7.488450E+00	3.655085E-01	-4.835245E-01	-3.307121E-01	-2.387133E+01

G R I D P O I N T F O R C E B A L A N C E

INT-ID	ELEMENT-ID	SOURCE	T1	T2	T3	R1	R2	R3
130		F-OF-SPC	0.0	0.0	0.0	-6.028096E+00	-3.447977E+00	9.246879E+00
130		APP-LOAD	0.0	1.200868E+01	0.0	0.0	0.0	0.0
130	9	QUAD4	-4.021852E+02	-9.345707E+02	4.014678E+03	5.592162E-01	1.767280E+00	9.034017E+00
130	10	QUAD4	3.776485E+02	8.928570E+02	-2.256225E+03	-4.806311E-01	-5.625299E-01	8.046698E+00
130	13	QUAD4	-5.888482E+02	-1.957212E+02	2.577555E+03	3.672503E+00	1.478331E+00	-1.349090E+01
130	14	QUAD4	6.133849E+02	2.254262E+02	-4.336008E+03	2.277008E+00	7.648961E-01	-1.283669E+01
130		*TOTALS*	-2.566765E-10	-6.753496E-10	7.958079E-11	-1.360023E-14	3.749778E-14	-8.482104E-14
131		APP-LOAD	0.0	1.198868E+01	0.0	0.0	0.0	0.0
131		F-OF-SPC	0.0	0.0	0.0	-4.270725E+00	6.266553E+00	2.769398E+01
131	13	QUAD4	-8.542455E+02	-3.374682E+02	1.521347E+04	2.216435E+00	8.753362E-01	-1.250562E+01
131	14	QUAD4	1.111672E+03	2.476562E+02	-1.285887E+04	-7.304964E+00	-3.244092E+00	-1.414690E+01
131	39	QUAD4	1.098397E+03	-7.226725E+02	1.474570E+04	6.163850E+00	-2.563097E+00	-1.318155E+00
131	40	QUAD4	-1.355823E+03	8.004958E+02	-1.710029E+04	3.195404E+00	-1.334700E+00	2.766990E-01
131		*TOTALS*	-3.515765E-11	1.162448E-11	-1.186891E-10	7.549517E-15	2.442491E-15	3.108624E-15
148		F-OF-SPC	0.0	0.0	8.845583E+03	-8.976212E-01	4.652664E-01	0.0
148		APP-LOAD	0.0	4.432799E+00	0.0	0.0	0.0	0.0
148	9	QUAD4	5.448954E+01	4.101875E+01	-3.895087E+03	-3.547052E-01	-9.891458E-01	-5.406407E-01
148	13	QUAD4	-5.448954E+01	-4.545155E+01	-4.950496E+03	1.252326E+00	5.238794E-01	5.406407E-01
148		*TOTALS*	1.510045E-10	2.188942E-10	-3.808509E-11	-5.523360E-15	-1.544598E-14	-1.915135E-13
150		APP-LOAD	0.0	2.238287E+01	0.0	0.0	0.0	0.0
150		F-OF-SPC	0.0	0.0	3.243218E+04	7.406997E+01	2.702240E+00	0.0
150	13	QUAD4	1.497583E+03	5.786409E+02	-1.284052E+04	-7.073768E+00	-2.953382E+00	-1.553995E+00
150	39	QUAD4	-8.315592E+02	1.349642E+03	-9.125044E+03	-1.792270E+00	3.646217E-01	2.092434E+00
150	139	QUAD4	6.818008E+03	-1.950667E+03	-1.046661E+04	-6.520393E+01	-1.134798E-01	-5.394384E-01
150		*TOTALS*	-2.535216E-11	-5.033485E-11	8.344614E-11	2.664535E-14	8.326673E-16	5.440093E-15

S T R E S S E S I N L A Y E R E D C O M P O S I T E E L E M E N T S (Q U A D 4)

EMENT ID	PLY ID	STRESSES IN FIBRE AND MATRIX DIRECTIONS NORMAL-1	NORMAL-2	SHEAR-12	INTER-LAMINAR STRESSES SHEAR-1Z	SHEAR-2Z	PRINCIPAL STRESSES (ZERO SHEAR) ANGLE	MAJOR	MINOR	MAX SHEAR
130	1	7.01630E+06	1.27938E+06	-1.28084E+06	-3.21319E+04	1.26435E+04	-12.03	7.28927E+06	1.00640E+06	3.14143E+06
130	2	1.55759E+07	8.59134E+05	1.27937E+06	-5.35532E+04	2.10724E+04	4.93	1.56863E+07	7.48742E+05	7.46876E+06
130	3	6.94419E+06	1.28299E+06	-1.27790E+06	-6.42638E+04	2.52869E+04	-12.15	7.21928E+06	1.00789E+06	3.10570E+06
130	4	1.56489E+07	8.55615E+05	1.27643E+06	-6.42638E+04	2.52869E+04	4.90	1.57582E+07	7.46286E+05	7.50597E+06
130	5	6.87209E+06	1.28659E+06	-1.27497E+06	-5.35532E+04	2.10724E+04	-12.27	7.14935E+06	1.00933E+06	3.07001E+06
130	6	1.57219E+07	8.52095E+05	1.27350E+06	-3.21319E+04	1.26435E+04	4.86	1.58302E+07	7.43818E+05	7.54319E+06
130	7	6.79998E+06	1.29020E+06	-1.27203E+06	2.72756E-03	-1.07326E-03	-12.39	7.07947E+06	1.01071E+06	3.03438E+06
131	1	-6.06379E+06	-3.80519E+04	1.03495E+06	1.09348E+04	5.53719E+03	80.52	1.34750E+05	-6.23660E+06	3.18567E+06
131	2	1.41239E+06	-4.04566E+05	-1.03474E+06	1.82247E+04	9.22864E+03	-24.36	1.88087E+06	-8.73045E+05	1.37696E+06
131	3	-6.07329E+06	-3.64464E+04	1.03452E+06	2.18697E+04	1.10744E+04	80.54	1.35916E+05	-6.24566E+06	3.19079E+06
131	4	1.43771E+06	-4.04671E+05	-1.03431E+06	2.18697E+04	1.10744E+04	-24.16	1.90158E+06	-8.68536E+05	1.38506E+06
131	5	-6.08279E+06	-3.48410E+04	1.03409E+06	1.82247E+04	9.22864E+03	80.56	1.37083E+05	-6.25472E+06	3.19590E+06
131	6	1.46303E+06	-4.04775E+05	-1.03388E+06	1.09348E+04	5.53719E+03	-23.95	1.92235E+06	-8.64096E+05	1.39322E+06
131	7	-6.09229E+06	-3.32355E+04	1.03366E+06	-9.28216E-04	-4.70031E-04	80.58	1.38251E+05	-6.26378E+06	3.20102E+06
148	1	1.65735E+06	1.50243E+05	1.43511E+06	-1.05371E+04	8.99464E+02	31.15	2.52472E+06	-7.17122E+05	1.62092E+06
148	2	1.55981E+06	1.55033E+05	-1.43511E+06	-1.75618E+04	1.49911E+03	-31.96	2.45520E+06	-7.40359E+05	1.59778E+06
148	3	1.65741E+06	1.50240E+05	1.43512E+06	-2.10742E+04	1.79893E+03	31.15	2.52477E+06	-7.17116E+05	1.62094E+06
148	4	1.55974E+06	1.55036E+05	-1.43512E+06	-2.10742E+04	1.79893E+03	-31.96	2.45516E+06	-7.40383E+05	1.59777E+06
148	5	1.65748E+06	1.50237E+05	1.43513E+06	-1.75618E+04	1.49911E+03	31.15	2.52482E+06	-7.17110E+05	1.62097E+06
148	6	1.55968E+06	1.55039E+05	-1.43513E+06	-1.05371E+04	8.99464E+02	-31.96	2.45513E+06	-7.40407E+05	1.59777E+06
148	7	1.65754E+06	1.50234E+05	1.43514E+06	8.94455E-04	-7.63521E-05	31.15	2.52488E+06	-7.17104E+05	1.62099E+06
150	1	3.68652E+05	-2.27929E+05	-5.85169E+05	1.11333E+04	-1.16205E+03	-31.49	7.27172E+05	-5.86449E+05	6.56810E+05
150	2	-3.33235E+06	-4.69138E+04	5.85168E+05	1.85554E+04	-1.93674E+03	80.20	5.41983E+04	-3.43346E+06	1.74383E+06
150	3	4.47443E+05	-2.33209E+05	-5.85167E+05	2.22665E+04	-2.32409E+03	-29.91	7.84052E+05	-5.69819E+05	6.76936E+05
150	4	-3.43074E+06	-4.34940E+04	5.85166E+05	2.22665E+04	-2.32409E+03	80.47	5.47474E+04	-3.52898E+06	1.79187E+06
150	5	5.26233E+05	-2.38489E+05	-5.85165E+05	1.85554E+04	-1.93674E+03	-28.42	8.42884E+05	-5.55140E+05	6.99012E+05

150	6	-3.52913E+06	-4.00741E+04	5.85164E+05	1.11333E+04	-1.16205E+03	80.73	5.54508E+04	-3.62466E+06	1.84005E+06
150	7	6.05023E+05	-2.43769E+05	-5.85163E+05	-9.45060E-04	9.86416E-05	-27.02	9.03488E+05	-5.42234E+05	7.22861E+05

F A I L U R E I N D I C E S F O R L A Y E R E D C O M P O S I T E E L E M E N T S (Q U A D 4)

EMENT ID	FAILURE THEORY	PLY ID	FP=FAILURE INDEX FOR PLY (DIRECT STRESSES)	FB=FAILURE INDEX FOR BONDING (INTER-LAMINAR STRESSES)	FAILURE INDEX FOR ELEMENT MAX OF FP,FB FOR ALL PLIES	FLAG
13	HOFFMAN	1	0.1404	0.0004		
		2	0.1379	0.0006		
		3	0.1429	0.0007		
		4	0.1335	0.0007		
		5	0.1455	0.0006		
		6	0.1292	0.0004		
		7	0.1482	0.1482		

S T R A I N S I N Q U A D R I L A T E R A L E L E M E N T S (Q U A D 4)

ENT).	STRAIN CURVATURE	STRAINS IN ELEMENT COORD SYSTEM NORMAL-X	NORMAL-Y	SHEAR-XY	PRINCIPAL STRAINS (ZERO SHEAR) ANGLE	MAJOR	MINOR	VON MISES
	-1.000000E+00	8.764486E-04	2.453991E-01	1.049576E-01	78.3847	2.561861E-01	-9.910560E-03	1.741882E-01

VECTOR RESULTANT

	T1	T2	T3	R1	R2	R3
1	-4.7235851E+00	-3.3648309E+02	-3.5573047E-01	1.6682791E+04	-8.7052994E+01	-1.6846219E+04